

ISSN 2219-6641

**SEISMOPROGNOSIS OBSERVATIONS
IN THE TERRITORY OF AZERBAIJAN**

Volume 18, № 1, 2020

<http://www.seismology.az/journal>

**Republican Seismic Survey Center of
Azerbaijan National Academy of Sciences**

**SEISMOPROGNOSIS OBSERVATIONS
IN THE TERRITORY OF AZERBAIJAN**

EDITORIAL BOARD

G.J.Yetirmishli (chief editor)
R.M.Aliguliyev (Baku, Azerbaijan)
F.A.Aliyev (Baku, Azerbaijan)
T.A.Aliyev (Baku, Azerbaijan)
F.A.Gadirov (Baku, Azerbaijan)
H.H.Guliyev (Baku, Azerbaijan)
I.S.Guliyev (Baku, Azerbaijan)
T.N.Kengerli (Baku, Azerbaijan)
P.Z.Mammadov (Baku, Azerbaijan)
T.Y. Mammadli (Baku, Azerbaijan)
H.O. Valiyev (Baku, Azerbaijan)

**INTERNATIONAL EDITORIAL
BOARD**

A.G.Aronov (Belarus)
T.L.Chelidze (Georgia)
Rengin Gok (USA)
Robert van der Hilst (USA Massa-
chusetts)
A.T.Ismayilzadeh (Germany)
R.Javanshir (Great Britain)
A.V.Kendzera (Ukraine)
A.A.Malovichko (Russia)
Robert Mellors (USA Livermore)
X.P.Metaxas (Greece)
E.A.Rogozhin (Russia)
Eric Sandvol (USA Missouri)
L.B.Slavina (Russia)
N.Turkelli (Turkey)

Responsible Secretary: Huseynova V.R.

MOHO DEPTH DETERMINATION BY CONVERTED PS-WAVE METHOD FOR THE TERRITORY OF THE GREAT CAUCASUS

Kazimova S.E.¹

Introduction

The first definitions of the depth of the surface of Mokhorovich in Azerbaijan were made on the basis of seismological data. Using the data from the DSS in compiling the gravitational model of the Earth's crust, the depth and accuracy of research have sharply increased. The DSS data provided the uniqueness of the solution of the inverse problem of gravimetry - the calculation of the depth density distribution. Most of the known methods of the automated approach involve obtaining a density section; the effect of which would coincide with the observed gravitational field.

The methodology of the reflected waves, or as it is commonly called, the "Receiver function" method, is well known and widely used throughout the world to study the deep structure of the Earth up to 800 km. The method is based on the registration, isolation, and interpretation of Ps-exchange waves. These studies were conducted as part of the International Seismotomographic Laboratory using a software package developed at the University of Missouri (USA). Studies in many countries of the world have shown the effectiveness of the method of reflected waves in studying the structure of the lithosphere within one or more seismic stations.

In the method of exchange reflected waves, the exchange waves propagate from the source as longitudinal, and at the boundaries in the area of the seismic station are transformed into transverse. To distinguish the phases of the reflected waves against random noise, it is necessary to know the properties of the converted waves and use them in the processing algorithm of the initial seismograms [6].

Passing the path from the exchange boundary to the surface at a lower speed compared to the refracted longitudinal wave P, the exchange waves Ps enter the records with some delay with respect to the wave P generating them. The delay time depends on the distance between the source and the station and the depth of the boundary at which the exchange took place. At a fixed exchange depth, the delay time of the exchange wave Ps decreases with increasing epicentral distance and increases with its decrease [6].

There are a number of criteria for recognition of exchange waves in seismograms. However, in practice, not all of them are kept. In particular, the sign of polarization is quite often not observed, that is, intense horizontal components of the "SH" components (perpendicular to the direction to the epicenter), often shifted in phase relative to the x "SV" components, are recorded [1, 3-5]. Since the transverse wave Ps in an isotropic medium is polarized as SV, the desired wave is emitted in the source – receiver plane in the direction perpendicular to the direction of polarization in the P wave (Fig. 1). Since the amplitude of the exchange wave Ps is much smaller than the amplitude of the P wave, the most critical moment of processing is the extraction of the signal of the exchange wave against the background of various waves and interference [6].

Data processing methods

Data processing consists of five main tasks: frequency filtering of input seismic records in the "SAC" format, rotation of the Z, N, E axes to the source, standardization of the L, Q, T components, obtaining individual receiving functions for each earthquake, summing traces from all earthquakes. Seismograms of selected earthquakes are processed using the Seismic Analysis Code (SAC) software package (developed by the University of Missouri (USA)) under the MacOS operating system.

¹ Republican Seismic Survey Center of Azerbaijan National Academy of Sciences

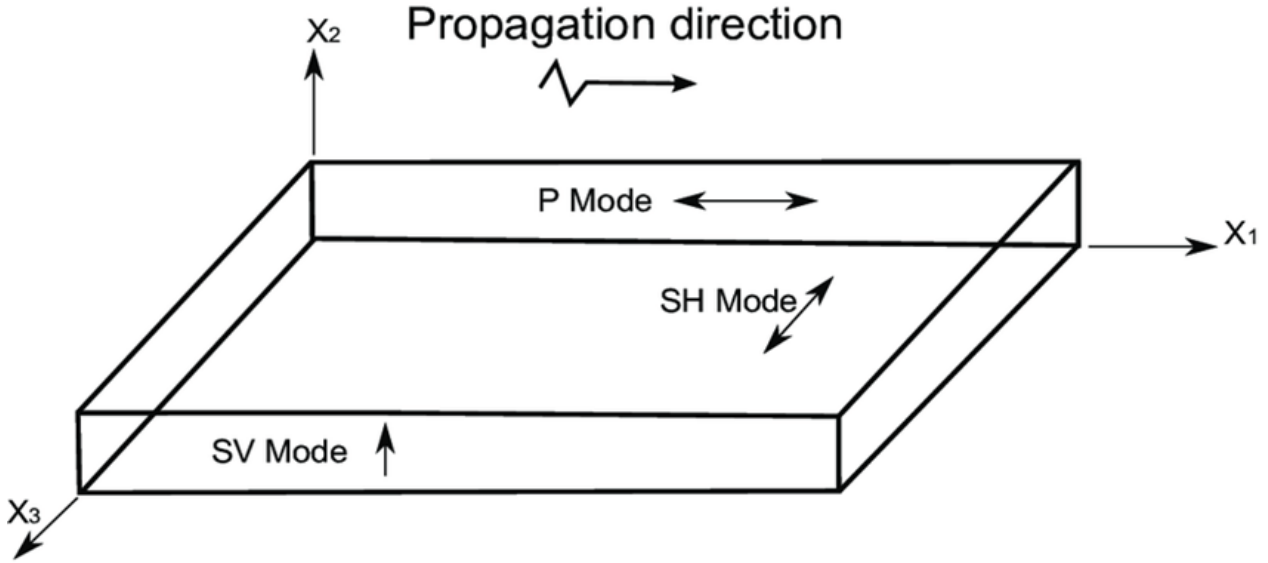


Figure 1. Three-dimensional coordinate system and polarization directions of waves P, SV and SH.

At the first stage, frequency filtering is carried out in order to eliminate oscillations that are too high, containing the effects of random scattering by inhomogeneities, and too low frequencies that reduce the resolution [6]. The working range of periods is from 2 to 10 seconds.

Next, two-dimensional and three-dimensional rotation of the axes. Mathematically, this transformation consists in finding the eigenvectors of the covariance matrix obtained by calculating the covariances of the vertical and radial components. Two-dimensional rotation of the axes can be represented in the form of a matrix [10]:

$$M_{2D} = \begin{bmatrix} \cos a & \sin a \\ -\sin a & \cos a \end{bmatrix} \begin{bmatrix} R \\ T \end{bmatrix} = M_{2D} \begin{bmatrix} N \\ E \end{bmatrix}$$

where N and E represent the original (horizontal) axis; R and T represent the radial and tangential components; α is the azimuth measured clockwise from the north.

Three-dimensional rotation of the axes is expressed as the following matrix [10]:

$$M_{3D} = \begin{bmatrix} \cos i & -\sin i \sin ba & -\sin i \cos ba \\ \sin i & \cos i \sin ba & \cos i \cos ba \\ 0 & -\cos ba & \sin ba \end{bmatrix}$$

$$\begin{bmatrix} L \\ Q \\ T \end{bmatrix} = M_{3D} \begin{bmatrix} Z \\ E \\ N \end{bmatrix}$$

where i is the angle of incidence, measured vertically; Z, E and N are the original (horizontal and vertical) axes; L, Q, and T are transformed axes: L corresponds to the direction of polarization of the P wave, Q is perpendicular to the axis of L and corresponds to the direction of polarization of the SV wave, T corresponds to the direction of polarization of the SH wave (Fig. 2).

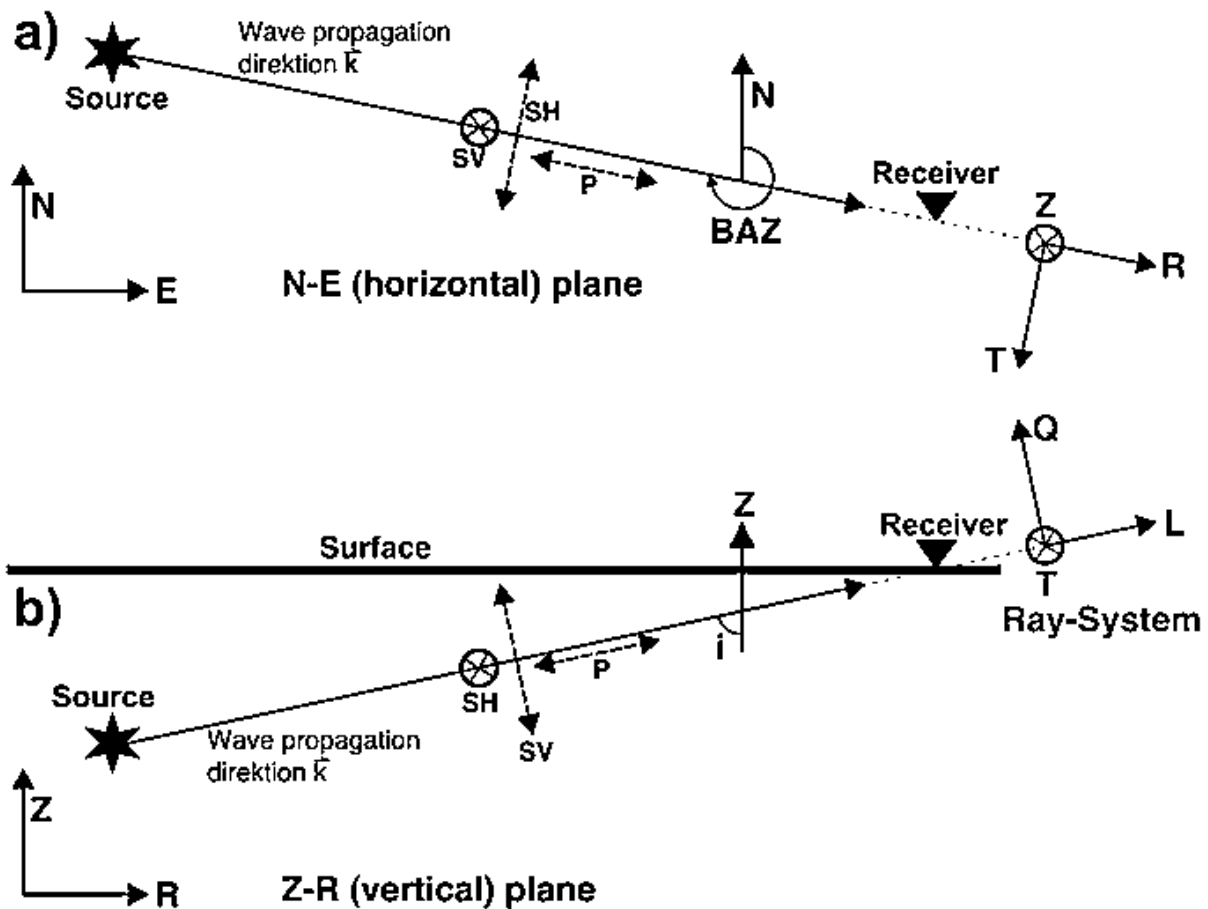


Figure 2. The motion of particles for waves P and S along the direction of wave propagation a) in the horizontal plane and b) in the vertical plane.

Application of the method of exchange reflected waves for the territory of the Greater Caucasus

One of the best regions for studying the early stages of mountain building is the Greater Caucasus, where most of the volcanism and mountain building is represented 5 million years. Of particular interest is the immersion zone of the Kura Depression under the Greater Caucasus, the so-called subduction zone, which has not been sufficiently studied up to date [8, 9]. To this end, we began our studies of the depth of the Moho border from this region. At the present stage, there is a dense network of highly sensitive digital seismic stations, which allows recording all seismic events with a magnitude of $m_l > 0.1$ within Azerbaijan, as well as remote telemetric seismic events around the world with $m_l > 5.0$. The study examined seismological data recorded by a network of telemetric stations ($N=20$) for 2009-2019 (Fig. 3). In total, 2428 earthquakes recorded at an epicenter distance of 35 to 90 degrees were analyzed. Remote earthquakes were taken to the "Earthquake Research Bureau" of the RSSC ANAS.

Thus, after filtering and rotating the seismic waves, the final components L, Q, T were standardized using a deconvolution filter formed on the section of the final seismogram containing the incident P-wave and part of its code (Fig. 4).

The subsequent processing operation was reduced to the summation of the standardized components of all earthquakes in order to suppress noise and release the exchange waves associated with various boundaries in the crust and mantle. The time of the exchange wave depends on the epicenter distance and is calculated for each path. The summation of all traces is carried out with time shifts relative to some reference epicentral distance, which is taken equal to 60 degrees. Figure

5 shows the summarized Q-traces of the receiving functions on which the Moho boundary with a delay time of 4.0 sec is clearly distinguished.

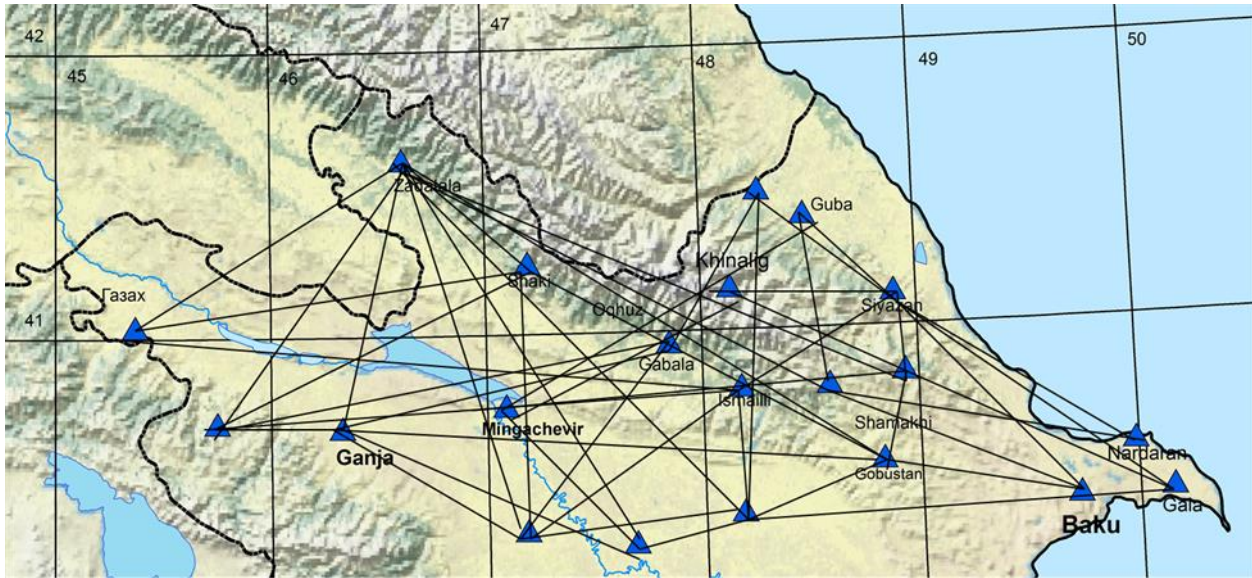


Figure 3. Network of seismic stations used in processing

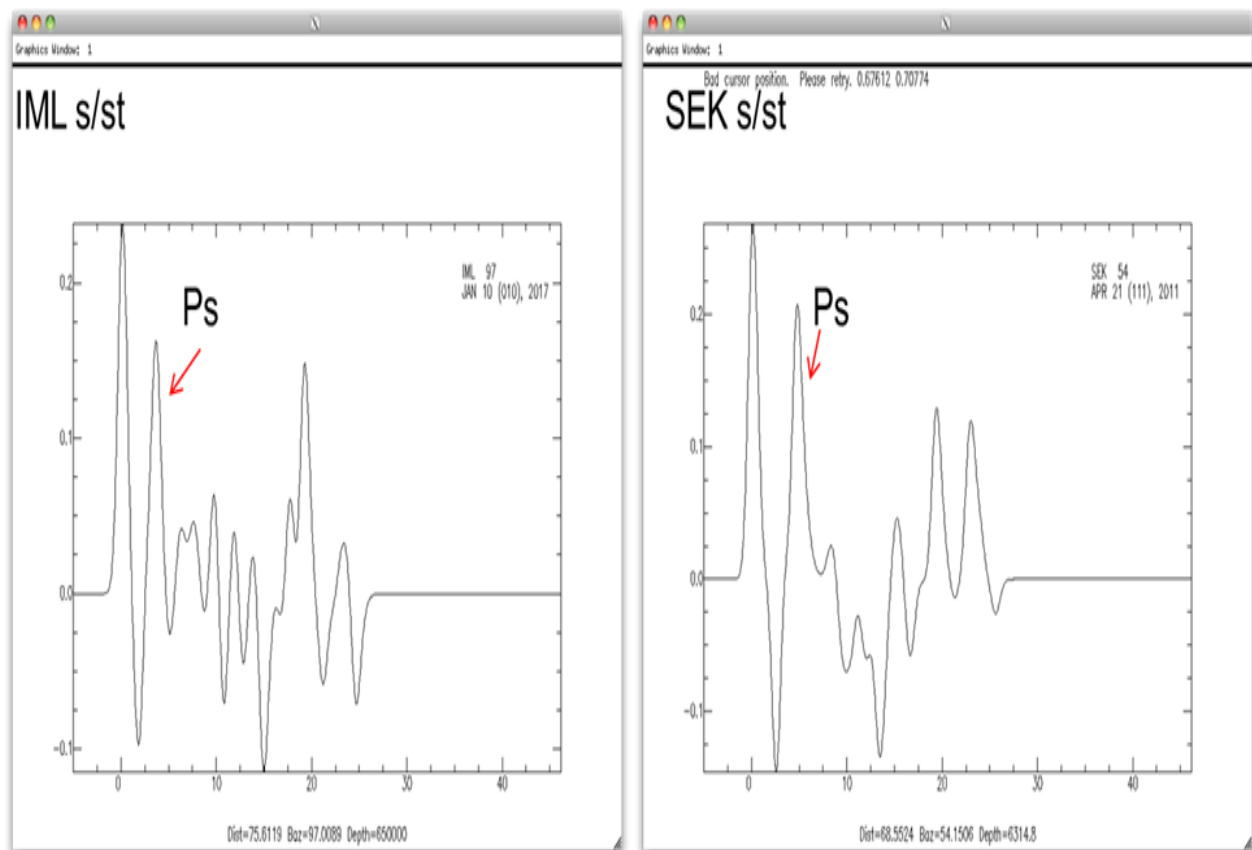


Figure 4. Standardized seismograms for the Ismayilli and Sheki seismic stations

Thus, having processed the data for all stations, the depths of the Moho border for the territory of the Greater Caucasus were calculated and a schematic map of isolines and a three-dimensional model were constructed (Fig. 6, 7).

Main conclusions:

For the first time, based on the analysis of the wave characteristics of distant earthquakes recorded at seismic and telemetric stations of the RSSC, the depths of the Moho border for the

Azerbaijan part of the Greater Caucasus were clarified by the method of exchange reflected Ps waves (receiver functions).

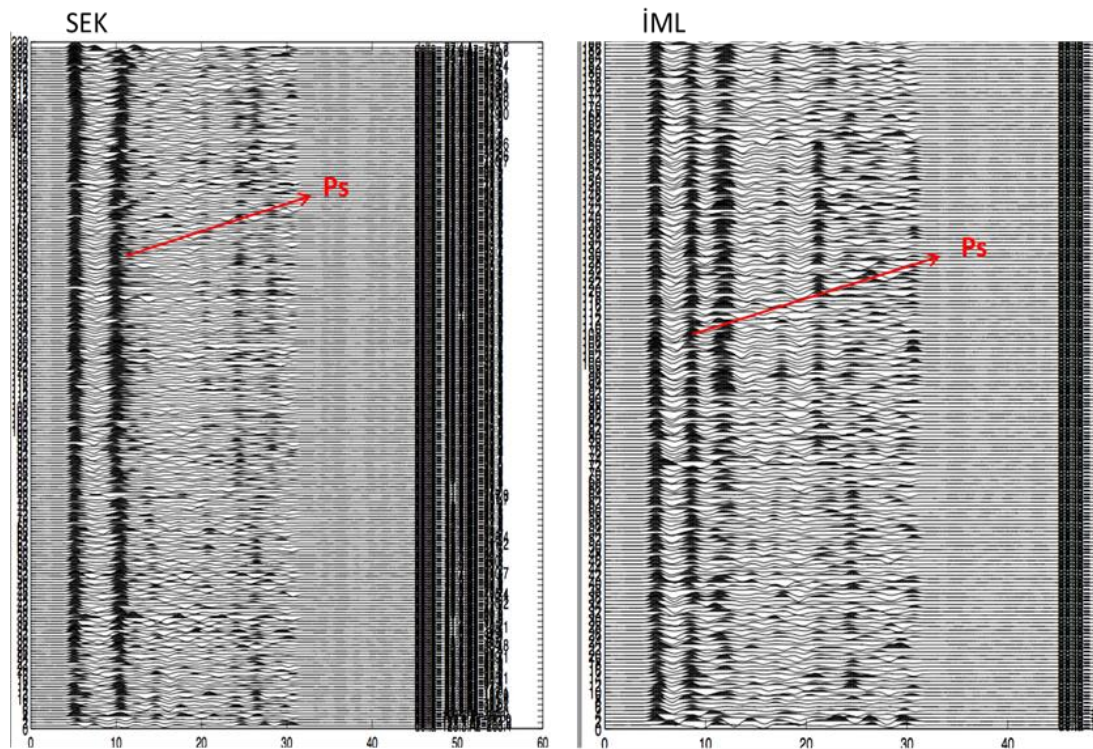


Figure 5. Summarized standardized components of all earthquakes for the Ismayilli and Sheki seismic stations

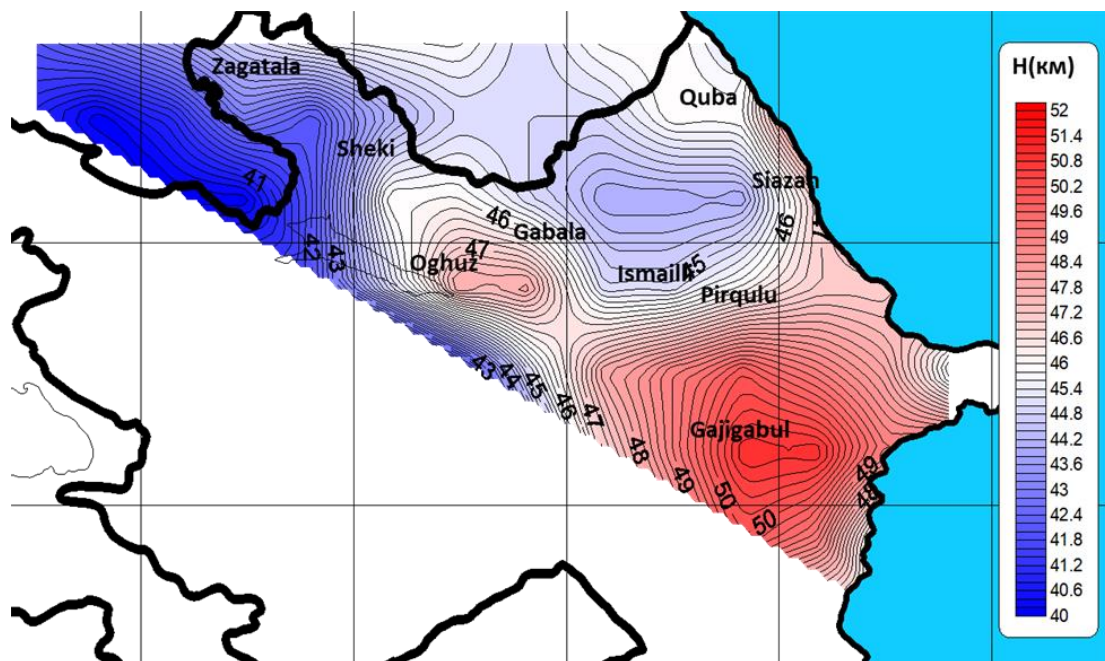


Figure 6. Map of contour lines of the Moho depth for the Greater Caucasus

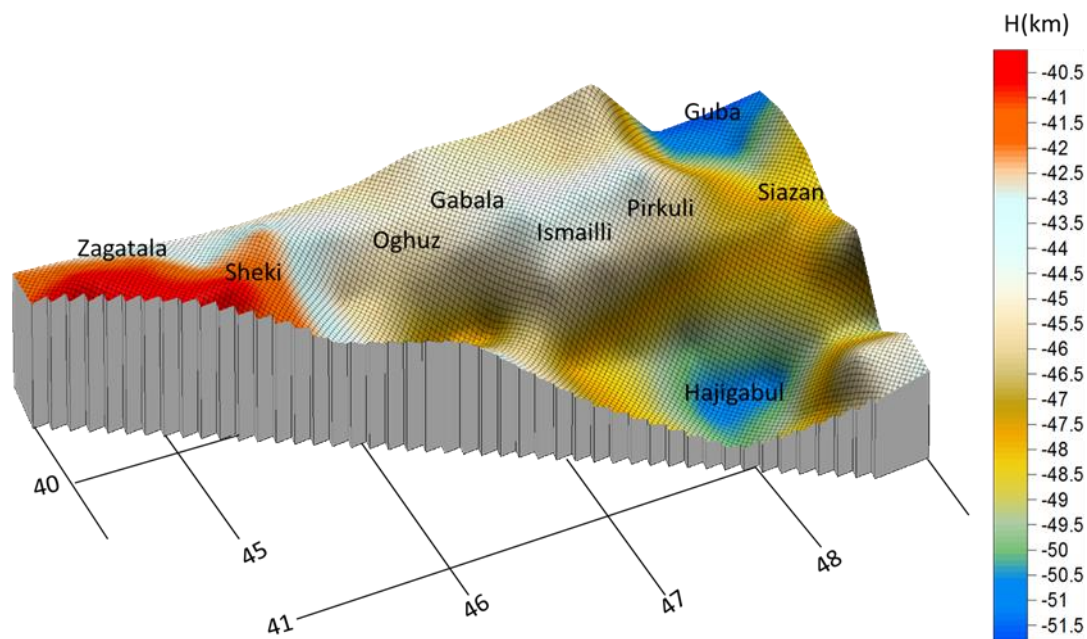


Figure 7. Three-dimensional model of the depth of Moho for the territory of the Greater Caucasus

Thus, a map of isolines of the depths of the Moho border was constructed and depths were determined for the territory of the Guba-Gusar region 48-50 km, the Zagatala-Balakan region 46-47 km, the Shamakhi-Ismayilli region 48-52 km. As it was said earlier, the first definitions of the depth of the surface of Mokhorovich in Azerbaijan were made on the basis of the data from the state earthquake and the gravitational model of the Earth's crust. Such models were built by Gadjiyev R.M. in 1965 and Shikhalibeyli E.Sh. in 1996. The data obtained are consistent with the available data, but discrepancies have been received. Compared with the map constructed according to the DSS-MCRW and gravimetry data (Gadjiyev R.M., 1965) [2] the difference in the thickness of the Earth's crust was from 1 to 15 km. Compared with the map constructed according to the DSV and gravimetry data (presented in the book by Shikhalibeyli E.Sh., 1996) [7], the difference in the thickness of the Earth's crust varied from 1 to 10 km.

REFERENCES

1. Булин Н.К., Трюфилькина Е.И. Использование обменных волн SP, регистрируемых при близких землетрясениях, для изучения глубинного строения земной коры. Изв. АН СССР. Сер. геофиз, 1960, №11, с. 1570-1579.
2. Гаджиев Р.М. Глубинное геологическое строение Азербайджана. - Б.: Азернешр, 1965, 200 с.
3. Егоркина Г.В. Азимутальные изменения скоростей сейсмических волн и трещиноватость горных пород Джавахетского нагорья // Изв. АН Арм. ССР. Науки о Земле. 1986. - Т. 39. - № Г - С. 3141.
4. Егоркина Г.В., Безгодков В.А., Егоркин А.А. Экспериментальное изучение анизотропии скоростей сейсмических волн в кристаллическом фундаменте // Вулканология и сейсмология. 1986. - № 4. -С. 49-58.
5. Егоркина Г.В., Безгоднов В.А. Изучение сейсмической анизотропии верхней части земной коры // Физика Земли. 1987. - № 4. - С. 2829.
6. Французова В. И., Ваганова Н. В., Юдахин Ф.Н., Винник Л.П., Косарев Г. Л., Орешин С.И. Строение литосферы по данным обменных волн под сейсмостанцией «КЛИМОВ-

СКАЯ», ГЕОФИЗИКА, ВЕСТНИК ВГУ, серия: Геология, 2011, № 1, январь–июнь, с. 176-183

7. Шихалибейли Э.Ш. Некоторые проблемные вопросы геологического строения и тектоники Азербайджана. - Баку: Элм, 1996, 215 с.

8. Kangarli T.N., Kadirov F.A., Yetirmishli G.J., Aliyev F.A., Kazimova S.E. andet. Recent geodynamics, active faults and earthquake focal mechanisms of the zone of pseudo subduction interaction between the Northern and Southern Caucasus microplates in the Southern slope of the Greater Caucasus (Azerbaijan), ISSN 2078-502X Geodynamics and tectonophysics Published by the institute of the Earth's crust Siberian branch of Russian academy of science 2018 Volume 9 Issue 4, p. 1099-1126

9. Yetirmishli G.J., Kazimova S.E. Modeling of the Earth's crust of the Greater Caucasus by Seismic Tomography, Innovations in minimization of natural and technological risks, Abstract of the first Eurasian Conference "RISK-2019", Baku, 2019, p. 117.

10. <https://service.iris.edu/irisws/rotation/docs/1/help/>

HYDROGEOLOGICAL CONDITION AND ITS IMPACT ON THE LEVEL OF SEISMIC HAZARD IN NIZAMI DISTRICT, BAKU CITY

Z.S.Aliyeva¹, L.T.Fettahova¹, F.Z.Mehdizadeh¹

Introduction. Seismicity of the construction site should be clarified during the construction of buildings, bridges and other civil and industrial facilities in the seismically active areas for the purpose of seismic safety of facilities.

Initially, the potential seismic hazard should be identified in the earthquake sources. In addition, engineer-seismological and hydrogeological conditions should be investigated in each construction site. Thus, major seismic hazard caused by strong earthquakes can change depending on the lithological composition, physical and mechanical parameters of the grounds located under the foundations of the facilities as well as hydrogeological conditions. In order to evaluate the effect of hydrogeological conditions on seismicity, the area of Nizami region, where numerous high buildings have been built in recent years and has sufficient engineer-seismological and hydrogeological data, was selected.

The formation of groundwater in the research area may occur due to infiltration of atmospheric precipitation, losses from sewerage pipelines, from irrigation systems, due to the proximity of the sea to the area during irrigation works are carried out. The level of water also depends on their nutrition regime and usage.

The water in Nizami district was very different in their physical and chemical composition and hydrodynamic conditions. Source of these waters:

1. Climate-dependent, that is, it associated with atmospheric precipitation and evaporation (condensation) (atmospheric precipitation increases in spring and autumn and it feeds groundwater)
2. It is associated with irrigation and separate waste water (household type) (during construction and in areas with developed infrastructure, grounds are artificially irrigated and so on this results in changes in the geological environment).
3. The areas in the northwestern part of Nizami are fed by salt water of the Great Shor Lake.

There are two types of groundwater in Nizami region:

1. Pressurized groundwater (artesian water)
2. Groundwater Large thicknesses, mainly waterlogged sand and low thickness (there are clay and limestone soils)

Based on fund materials, a total of 1560 wells were drilled in construction sites (mainly in the eastern part of Nizami district). Depth of the well varies (10m, 30m, 60m and 120m). According to the research, the level of the groundwater is between 5,0 and 10,0 meters at H.Aliyev Avenue 105, 109, 111 and on 2 Kondalan Avenue intersecting with H.Aliyev Avenue. Along with groundwater in this area, pressure water horizons were found at depths of 12,0-30,0m; 38,0-50,0m; 52,0-63,0m and 79.0-92.0 m.

As can be seen from Figure1, the lithological composition of the ground in the areas where artesian water is widespread is very diverse: they are contain sandy, hard plastic clay and shelly limestone. The thickness of this complex is more than 60 meters.

The Artesian water is located in the north-west of the region as we mentioned above. Artesian water is the confined natural underground reservoir that contains water under positive pressure (sands, fractured limestone, sandstone, karstic soils).

Mineralization of water is high due to its proximity to the Great Shor Lake. As a result of circulation in salty rocks, the water gets richer with salt. The sope level of artesian water is located below the groundwater level and artesian pool is formed. Soil can contain gypsum and various water-soluble salts. Dissolution of salts in water causes suffocation or washing away water from the

¹ Republican Seismic Survey Center of Azerbaijan National Academy of Sciences

field. As a result, there are gaps in the ground and the uneven impact of the building to the foundation resulting in the collapse of the ground.

Artesian water can rise from the ceiling of the aquifer to the surface and sometimes can form a fountain. It is likely that if construction is carried out in these areas in the future, then as a result of human activities or the weight of the buildings under construction. The underground rocks will be damaged and destroyed by pressure water, as a result, it adversely affects the seismic properties of these rocks and leads to the collapse of buildings. Even in areas where artesian water is found, it is also very dangerous to fix the underground rocks of the constructed buildings with piles. Such areas are unsuitable for construction.

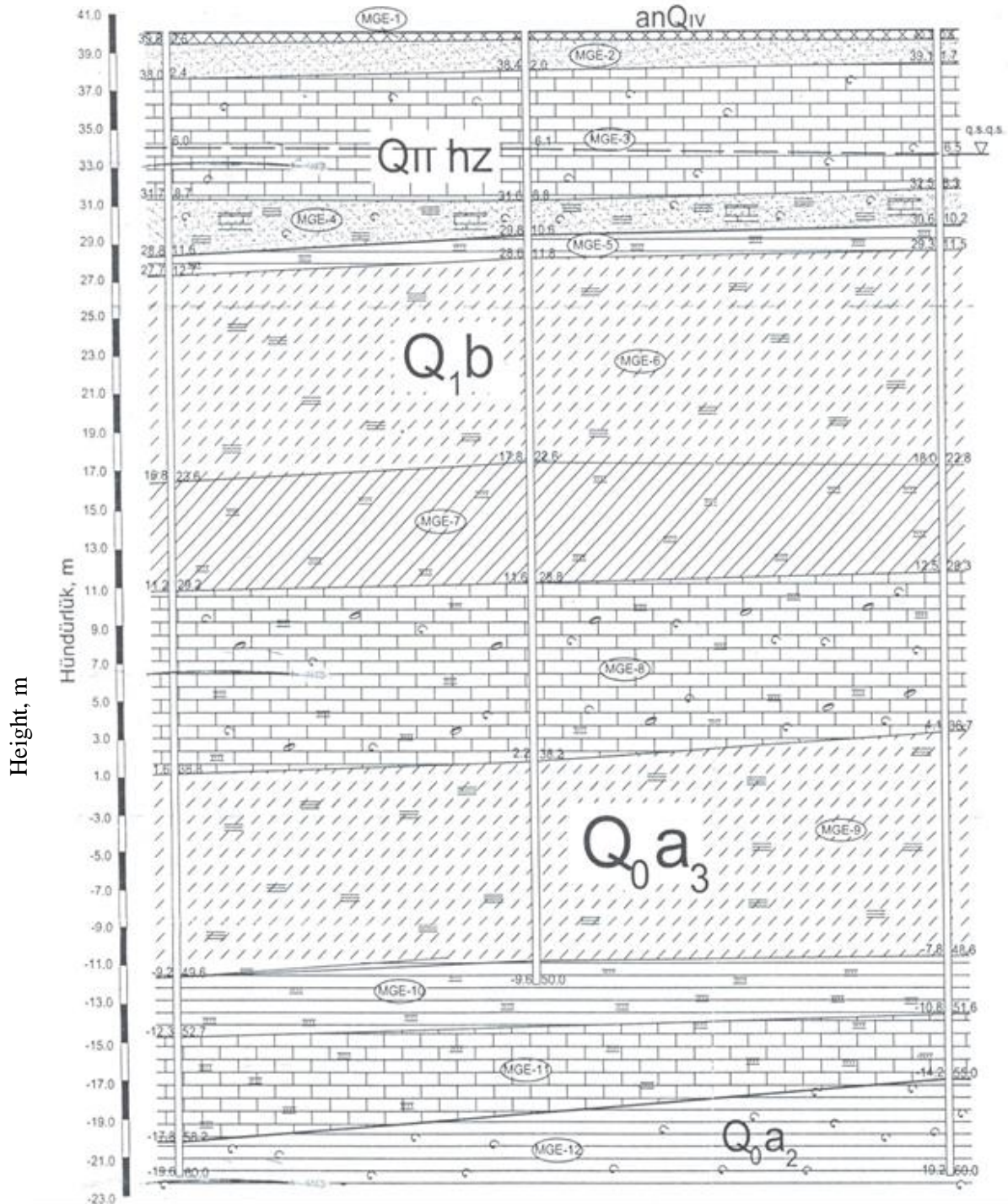


Figure 1. Example of geological-lithological section of the area where there is artesian water.

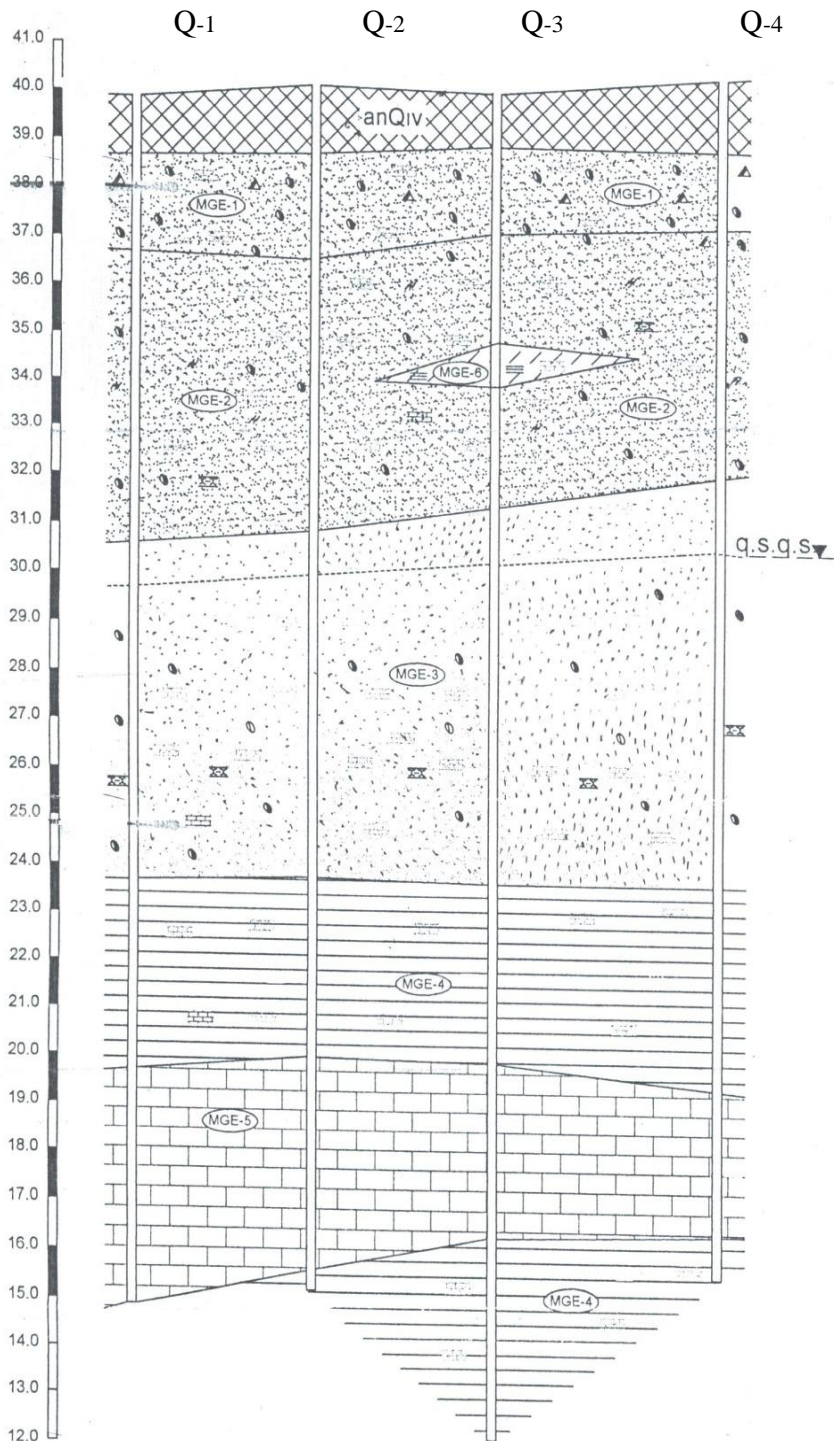
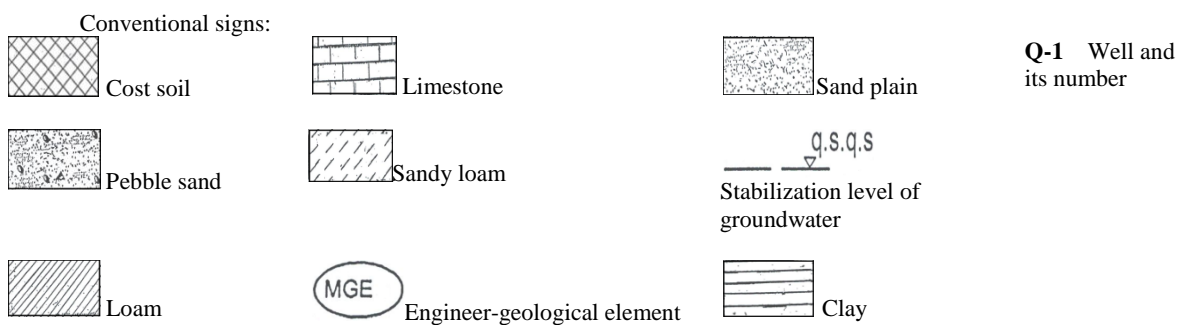


Figure 2. Example of geological-lithological section of the area with high seismicity (point)



Water is almost a permanent component of rocks. Groundwater is constantly in motion, that is, the regime changes and it has a great effect on rocks, especially clay soils, due to its chemical activity and this drastically changes their properties and as a result, it leads to consolidation or thinning of the soils (thixotropy). As the composition of groundwater is variable, their impact on rocks also changes (Zaalishvili, 2014).

We encounter such conditions at construction sites located in the north-eastern part of Nizami district.

Unpressurized groundwater in this area is very diverse, widespread and unevenly distributed. Water is characterized by the level of formation, mineralization and chemical composition. The chemical composition of groundwater has a significant effect on the swelling of clays. Groundwater is mainly found in cast soil and watery sandy ground with large thickness in the areas located in blocks numbered 2402, 2566 and 2399 and moreover V.Aliyev str. 26, at the crossing of Qara Qarayev pr. and Nakhchivanski Street and at the Babek Avenue (Fig. 2).

The width (V_s) of the soils involved in geological sections is determined by the class of wave propagation, and if there are soils saturated with water or prone to liquefaction in the area, the seismicity of the construction site is rated high (Fig. 3). In these wet grounds, the velocity of seismic waves is about 300m/s or less.

The remaining areas are low seismicity (point) areas. As can be seen from the crossings, low-thickness groundwater is found in other areas. Aquifers were found at different depths for the area, but no groundwater was found at several construction sites. In most places, water has low mineralization and the mineralization of water varies in the range of 1.1-4.5 g / l.

The degree of mineralization of groundwater depends on their level. As water levels fall, their mineralization decreases and their chemical composition changes (Projected buildings..., 1998-2018).

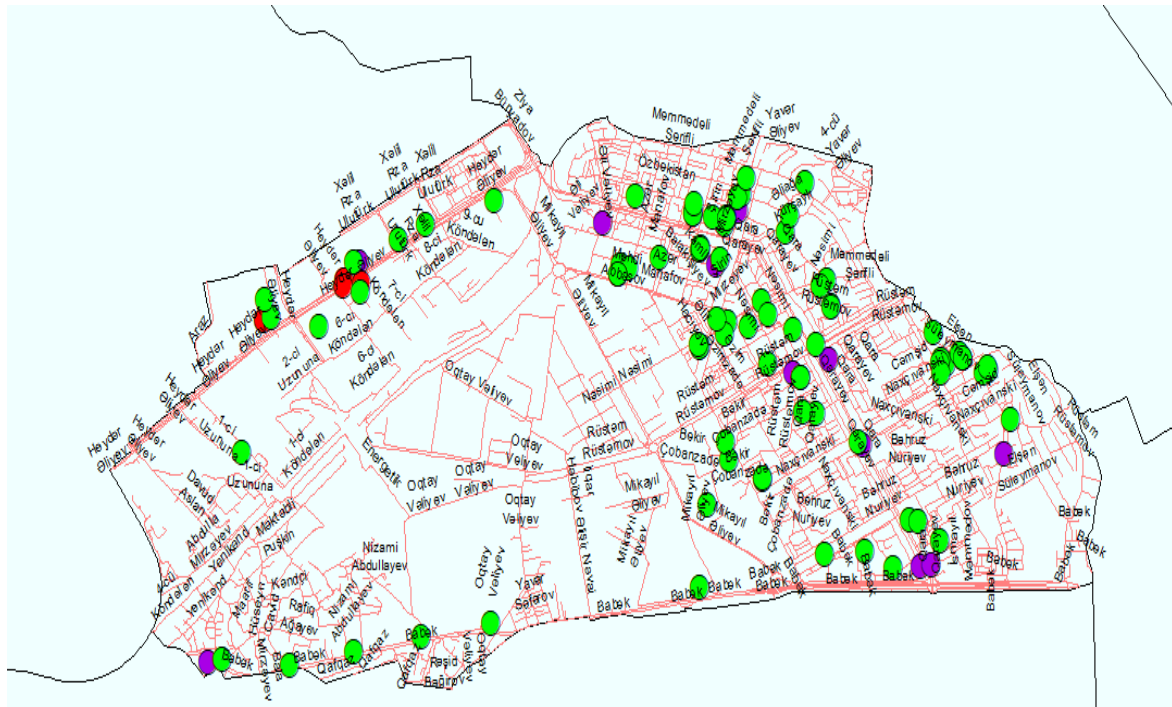


Figure 3. Map of seismic hazard assessment based on hydrogeological conditions in Nizami district

Symbols:

- - areas where artesian water is available
- - areas with high points
- - suitable areas for construction

Conclusion:

There are 2 types of pressurized groundwater - artesian water and groundwater in Nizami district. Artesian waters are located in the northwest of the region near the Great Shor Lake. This is a very dangerous situation for the area, which can be a problem for construction sites and is considered an unfavorable area.

In the north-eastern part of Nizami district, unpressurized groundwater is found. These waters are mainly formed in moist and water-saturated sandy soils with a large thickness. The seismicity of the area is rated high.

In the rest, groundwater is found at different depths and is less thick. This part is rated lower than the above areas.

REFERENCES

1. В.Б. Заалишвили. Некоторые проблемы практической реализации сейсмического микрорайонирования, факторы, формирующие интенсивность землетрясения, Владикавказ, 2012, Геология и геофизика Юга России, № 3, 2014
2. Layihələndirilən binaların, qurğuların tikintisi üçün ayrılmış sahələrin seysmik balının dəqiqləşdirilməsi haqqında hesabatlar. AMEA nəzdində RSXM-nın fondu 1998-2018-cu illər.
3. “Seysmik rayonlarda tikinti Az DTN 2.3-1”, AR Dövlət Şəhərsalma və Arxitektura Komitəsi, Bakı – 2009.
4. Справочное руководство гидрогеологии под редакцией проф. В.М. Максимова, Том 1, 2., Ленинград “Недра”, 1979.

SEISMICITY OF ZAGATALA TERRITORY FOR 2019

S.S. Ismayilova¹, E.S. Garaveliyev¹

Seismological studies

The Zagatala-Balakan zone is one of the main seismic active zones in Azerbaijan. Tectonically, the Zagatala-Balakan seismic active zone is located in the north-western part of the Azerbaijani part of the Greater Caucasus.

Strong and tangible earthquakes have been occurred in the seismic zone in the past and modern times. The first information about the earthquake in this area dates back to 1880. In 1936, so far registered in this zone there was the most powerful earthquake of 5,6 points. The intensity of the earthquake at the epicenter was 7 point (according to 12 points of 64-MSK scale). A map of the epicenters of historical earthquakes in the studied area has been shown in the Figure 1.

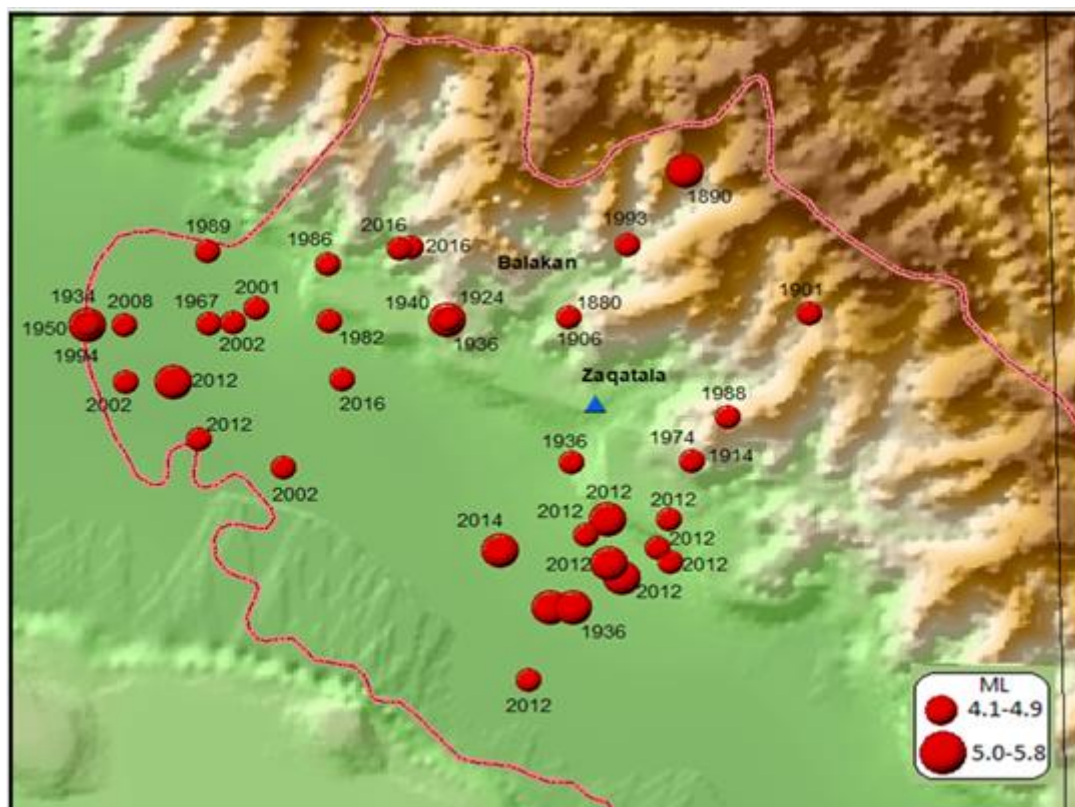


Figure 1. The map of the epicenters of historical earthquakes occurred in the studied area

Two shocks that occurred in Zagatala on May 7, 2012, with a time difference of 10 hours apart played a special role in terms of seismotectonic and engineering-seismological study of the area. The magnitude of the first shock was 5.6, depth was 8 km and the magnitude of the second shock was 5.7, depth was 12 km. The intensity of both shocks at the epicenter was 7 points (according to 12 points of 64-MSK scale).

After these earthquakes, several strong earthquakes have been recorded in the Zagatala zone. The last strong earthquake in the area has been recorded on August 10, 2019, at 13:35 local time, in the 18 km south-west of Zagatala station. The magnitude of the earthquake was 4.9, the depth was $h=5$ km.

In order to investigate the area seismotectonically, the distribution of faults and earthquakes in Balakan-Zagatala, Sheki, Gabala regions has been studied. As can be seen from the map,

¹ Republican Seismic Survey Center of Azerbaijan National Academy of Sciences

earthquakes in the Zagatala area and adjacent areas are located at the section zone of the depth faults in different directions (Fig. 2)

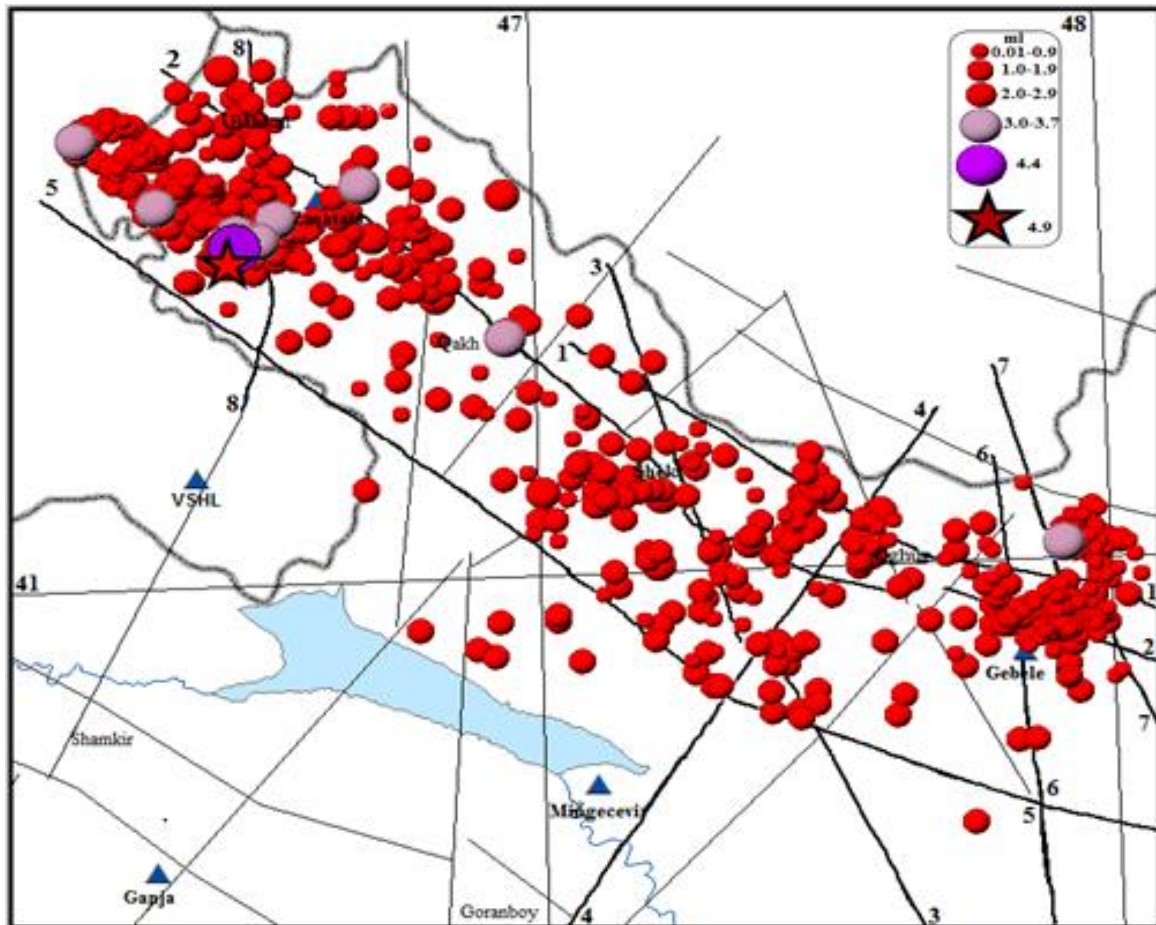


Figure 2. Map of epicenters of the earthquakes occurred in the Zagatala-Gabala region on faults. Faults: 1. Dashgil-Mudrese 2. Vandam (lengthwise) 3. Akhvay (orthogonal) 4. Tartar-Oghuz (transverse) 5. Alazan-Ayrichay (lengthwise) 6. Chakhirli-Gabala (orthogonal) 7. Ismayilli-Sighirli (orthogonal) 8. Sharur-Zagatala (transverse) (Author of faults: T.N.Kangarli)

A seismic transect has been constructed along the Balakan-Gabala I-I profile passing through the seismically active zone of Azerbaijan. The profile extends in all-Caucasian direction along the Ayrichay-Alat deep fault (Fig.3)

There are many hypocenters in the north-west of the section in the Zagatala-Balakan area. Earthquakes of magnitude mainly 0.01 had been occurred in the area. In contrast to 2018, an increase in earthquakes with a magnitude of ml 3.0 have been observed during the year, with the hypocenters located mainly at depths of 2-30 km. Earthquakes with a magnitude of 3.0 have been occurred within the sedimentary layer at a depth of 7-11 km. The epicenters were located in the effect zone of the depth faults in Vandam and Sharur. It is observed that the seismicity in Sheki and Gabala zones in the south-eastern part of section is weak and hypocenters are at a depth of 2-40 km.

Analysis of the number of earthquakes in the Zagatala zone in 2019 and the distribution of the seismic energy by months shows that the seismicity was below the background level at the beginning of the year and the number of earthquakes increased from July to September. In August, there was a sharp rise in seismic energy. The high seismic energy is due to the occurrence of earthquakes with a magnitude of 3.0 in this area. Starting in October, a decrease in the number of earthquakes and seismic energy was observed and the seismicity fell down below the background level (Fig. 4).

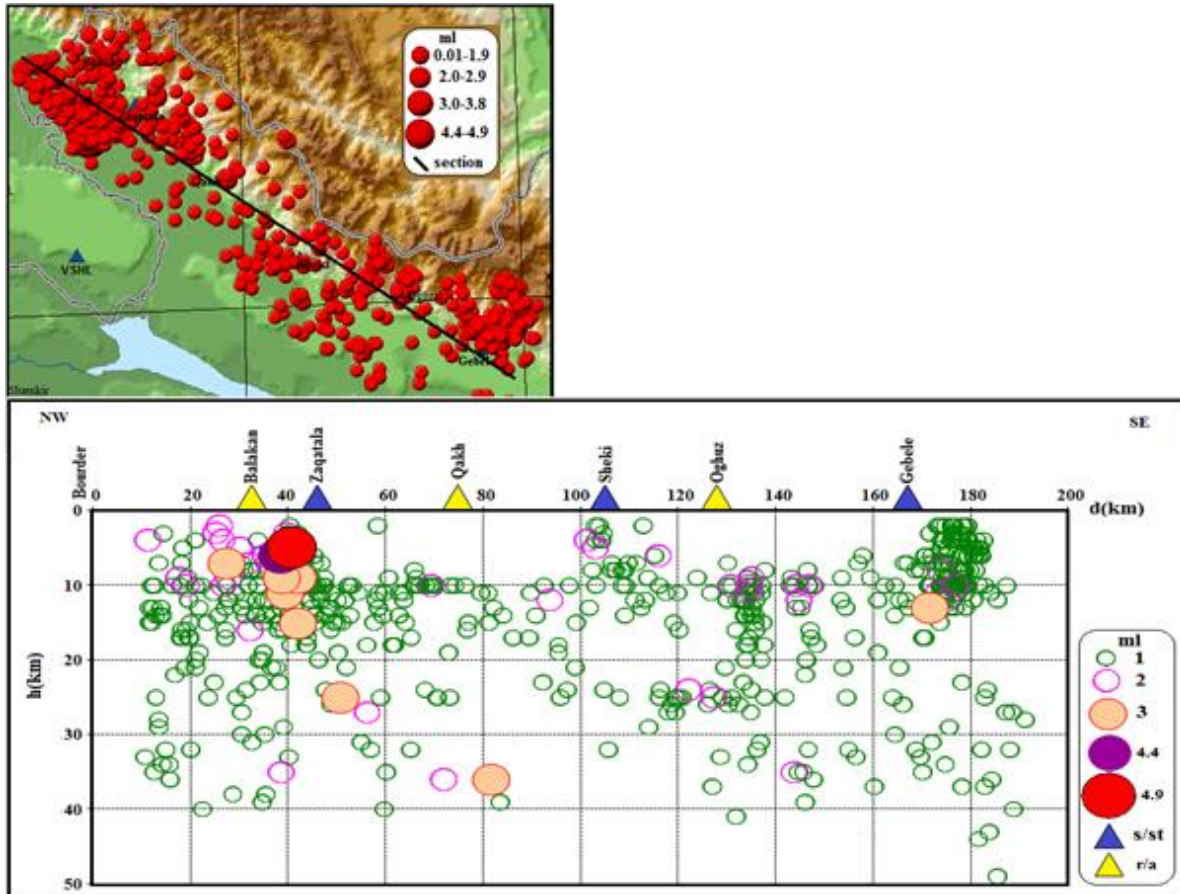


Figure 3. Seismological transect on I-I profile of Zagatala-Balakan Gabala zone

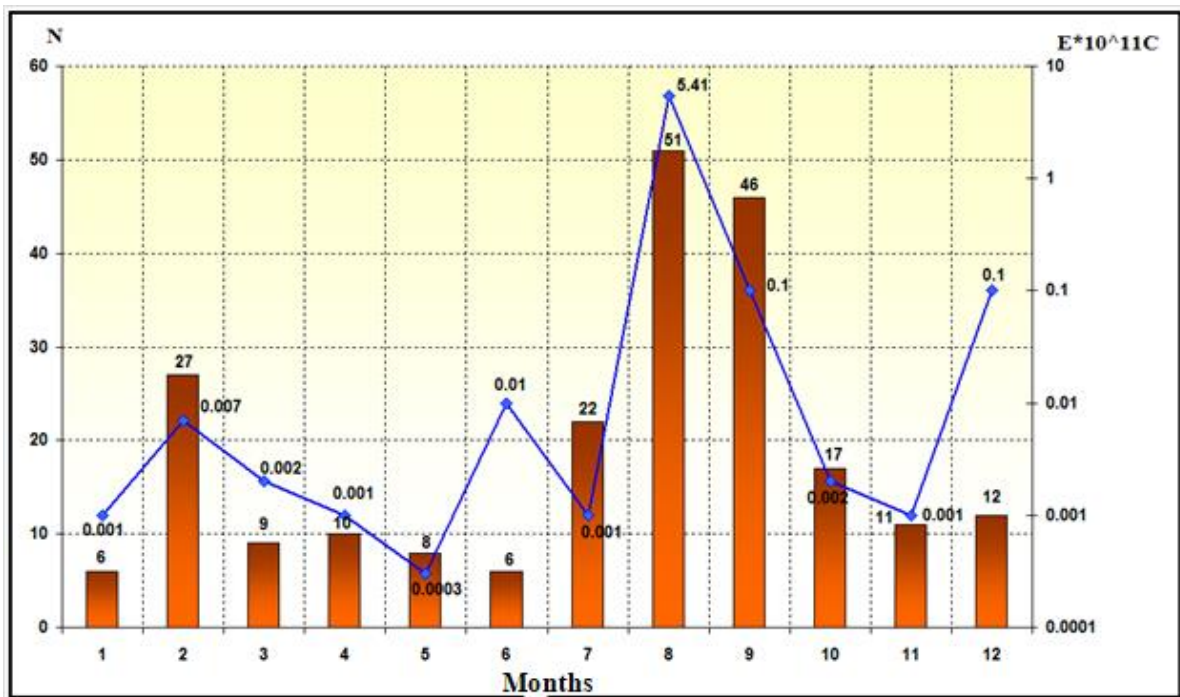


Figure 4. Histogram of the number of earthquakes in the Zagatala zone and the distribution of seismic energy by months.

Macroseismic studies

The earthquake with the highest intensity (magnitude of 4.9) in Zagatala has been occurred on August 10, 2019. The epicenter of the earthquake was located near the village of Danachi, Zagatala region, at a distance of about 3 km.

During the earthquake, people felt a strong shock and they fled to the yard in fear. There are houses damaged and unrepaired after the Zagatala earthquake on May 7, 2012 in the settlements near the epicenters of the region. During the earthquake, the cracks in many of those houses widened. In the village of Makov, a damaged wall of a house collapsed. There were almost no complications in the newly built houses. Based on materials collected from 22 settlements in the country, it was determined that the earthquake was felt at a magnitude of 6 at the epicenter, the geometric dimensions of the Pleistocene area were 14x16 km and the macroseismic area generally has an extension in the direction of the Greater Caucasus.



Figure 5. The collapse of the river stone wall of a house in the village of Makov



Figure 6. Old and new cracks on the wall of a house in Goyam village



Figure 7. Old and new cracks on the wall of a house in Goyam village

Schedule 1.

Macroseismic data of the Zagatala earthquake on August 10, 2020

№	Names of settlements and corresponding intensity, points	Epicentral distance, km	№	Names of settlements and corresponding intensity, points	Epicentral distance, km
6			4		
1	Danachi	3.0	13	Kadula	67.0
2	Makov	5.0	14	Sheki	71.5
3	Gamishtala	7.5	15	Goybulagh	81.0
4	Ititala	8.0	16	Dakhna	83.0
5	Ali Bayramlı	8.0	17	Shamkhir	89.0
5			3		
6	Mughanli	11.0	18	Balaken	18.0
7	Goyam	14.0	19	Gyulluk	26.0
8	Katekh	13.0	20	Kakhi	42.5
9	Shambulbina	16.5	21	Garatala	43.5
10	Zakatali	18.0	22	Salahli	49.5
11	Aliabad	20.0			
12	Yeni Suvagil	22.0			

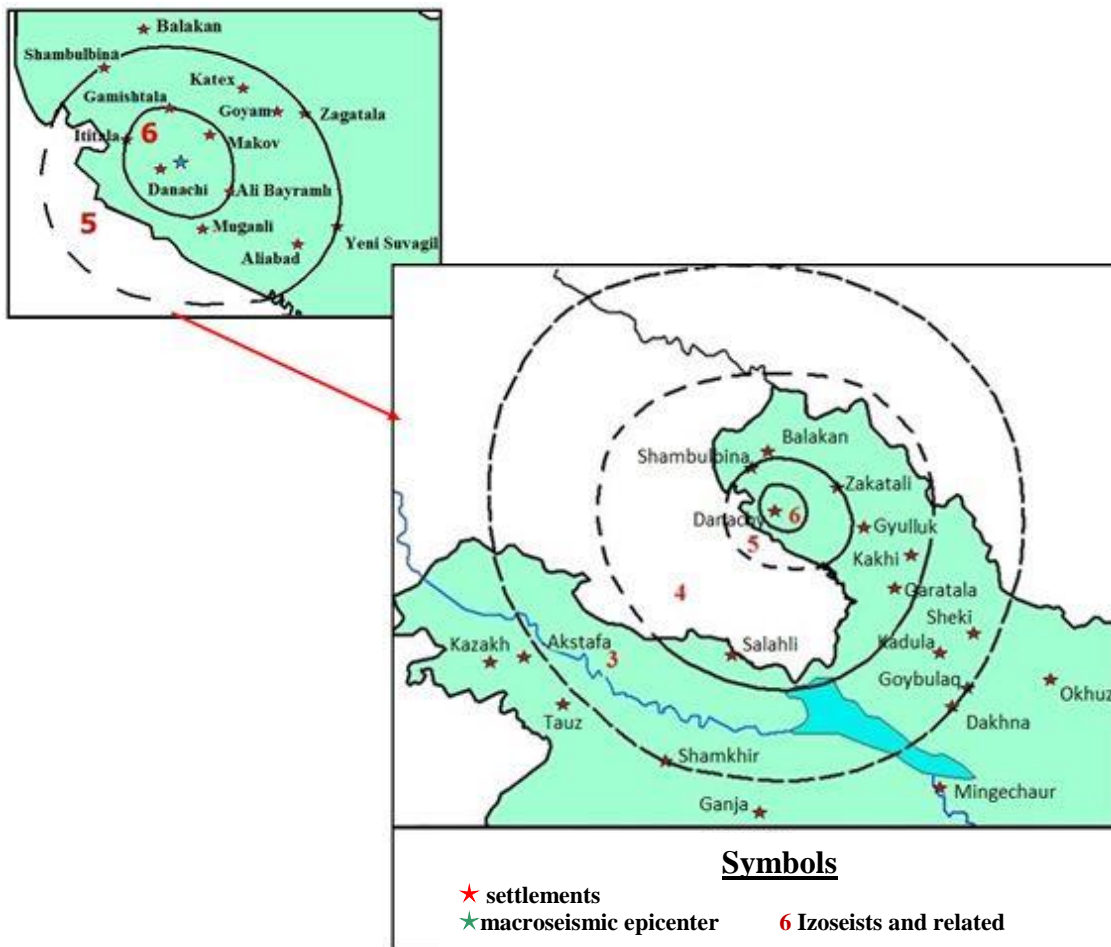


Figure 8. Macroseismic area of the Zagatala earthquake occurred on August 10, 2019

Conclusion

- It has been determined that the sources of the earthquake in the Zagatala zone were located in the effect zone of the Vandam and Sharur-Zagatala depth faults and the earthquakes with a magnitude of 3 were located within the sedimentary layer .
- In 2019, compared to 2018, seismicity have been higher than the background level. The number of earthquakes with a magnitude of ml 3 have been increased and the $\sum E=5.64 \times 10^{11}$ C release of energy from the Earth's crust during the year has been determined.
- It has been determined that the geometric dimensions of the Pleistocene area of the earthquake were 14x16 km, the intensity was 6 points in the epicenter and macroseismic area of the earthquake was extended in direction of the Greater Caucasus.

REFERENCES

1. Новый каталог сильных землетрясений на территории СССР Отв. редактор Н.В.Кондорская, Н.В.Шебалин. М.:Наука, 1977.

FEATURES OF CHANGE OF SEISMOMAGNETIC EFFECTS BEFORE THE STRONG IMISHLI EARTHQUAKE OCCURRED IN THE MIDDLE KURA DEPRESSION IN 2016

N.B. Khanbabayev¹

Researchers know that the geomagnetic effects are observed with anomalous changes caused by strong earthquakes in the seismoactive areas. The collected information is regularly studied in geodynamic polygons of the world and in Azerbaijan with modern magnetometric devices.

Comparative analysis of available data and experience of previous researches in magnetometric polygons established in several regions of the world - China, Russia, Uzbekistan, Kazakhstan and Tajikistan have allowed the magnetometric observation method to be considered as one of the earthquake warning factors [1].

The accumulation of the stress-strain energy at different depths of the Earth's crust is related to both local and cosmogenic factors. Mechanical, physico-chemical and other features of the environment change with characteristic indicators in the source of the earthquakes which occurred in Middle and Lower Kura depression, the northern and southern slopes of the Greater Caucasus, the Azerbaijani sector of the Caspian Sea where the anomalous stress-strain energy is accumulated and effects of such active processes on the Earth's surface are studied in the seismic regions of the world as warning factors of geophysical fields: earthquakes, gravitational, electrical, magnetic and geochemical abnormal changes [1,2].

The epicenter map of the earthquakes occurred in the Middle Kura depression and adjacent areas during 2004-2016 years is given below.

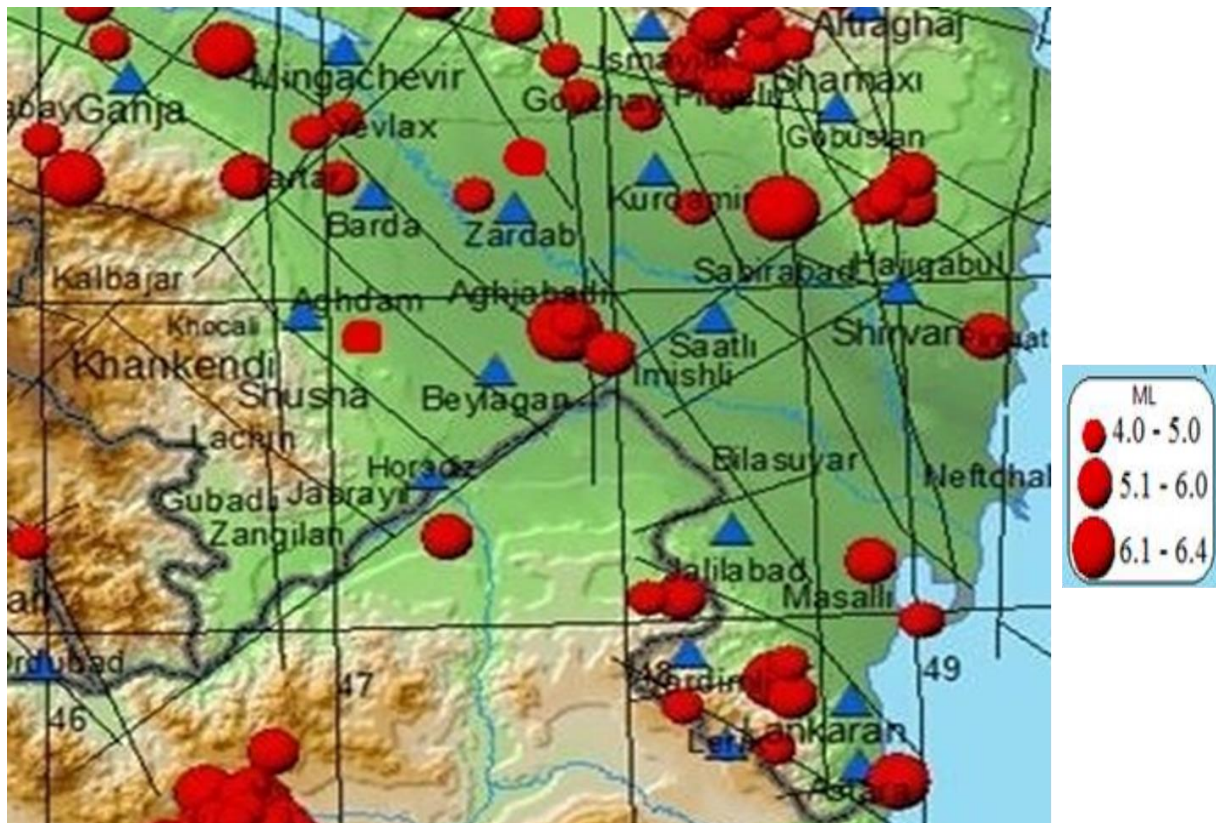


Figure 1. Epicenter map of earthquakes occurred in the Middle Kura and adjacent areas during 2004-2016 years.

1967 shocks have been recorded in the 3rd quarter of 2016 year in the Middle Kura depression. The amount of seismic energy was $E=55 \cdot 10^{11}$ C. The amount of seismic energy during

¹ Republican Seismic Survey Center of Azerbaijan National Academy of Sciences

the quarter of 2016 was higher than in the previous quarters. The reason of this was the strong earthquake occurred ($m=5.6$) in the Imishli region on 01.08.2016 year.[6]

The earthquake has been felt at 5 point in the epicenter and up to 5-3 point in the surrounding areas. This earthquake has been accompanied by a small number of aftershocks. Three of these earthquakes have been felt.

Seismicity in the Middle Kura depression was higher than the background level. Epicenter of Imishli earthquake and its aftershocks are located in the Kura-Caucasus and Gabala-Chakhirli orthogonal tension zones.

Imishli and Sabirabad earthquakes sources are known in these parts of the Middle Kura depression. In 2016, the geodynamic activity of the Imishli zone has been greater than that of the other regions.

In previous years, earthquakes with magnitude 4 have been recorded in the Imishli source zone on the map of strong historical earthquakes (427-2016 years). Two of these are earthquakes of magnitude 6 in the 1862 and 1934 years. [6]

The parameters of historical earthquakes in Imishli region have been shown in Table 1.

Table 1

№	Year	Month	Day	Time	lat	lon	H	ml	Point	Note
1	1862	12	19	02-30±1	39,70	47,90	25	6,4	7	Imishli
2	1911	6	23	12-30-19	40,00	48,00	18	5,6	6-7	Imishli
3	1916	5	14	12-11±1	40,00	48,10	30	5,6	5	Imishli
4	1934	10	29	16-15-45	39,90	47,80	30	6,3	6-7	Imishli
5	1959	8	13	00-33-11	39,90	48,20	12	5,3	6-7	Imishli
6	1964	11	9	08-05-48.0	39,80	48,20	14	5,3	6	Imishli
7	1965	5	15	18-43-05.0	39,90	48,00	10	4,6	6	Imishli
8	1968	6	24	18-28-44.0	40,00	48,10	15	4,6	5	Imishli
9	1975	12	16	07-42-50.0	39,70	48,10		4,5		Imishli
10	1976	2	3	16-40-40.5	40,00	48,10	7	5,4		Imishli
11	1999	6	4	11-56-58.2	40,02	48,22	37	4,2		Imishli
12	2016	8	1	4:46:35.799	39,91	47,85	28	5,6	5	Imishli
13	2016	8	1	7:51:01.571	39,92	47,87	25	4,1	3	Imishli
14	2016	10	16	7:52:20.874	39,83	48,00	21	4,4	4	Imishli

The compressive strain of the earthquake magnitude of 5.6, occurred in Imishli area in the 01.08.2016 year is north-east ($AZM=47^\circ$) oriented, close to the horizon ($PL_P=18^\circ-70^\circ$) and tension strain is south-west oriented ($AZM=254^\circ$), ($PL_P=70^\circ$). The displacement element of the type of movement for both sharp flatness ($DP_1=65^\circ$, $DP_2=28^\circ$) is reverse fault. For NP1 modal flatness ($STK_1=324^\circ$), the movement is with the north-west direction and for NP2 modal flatness ($STK_2=123^\circ$), it is with the south-east direction. The earthquake source is located in the Kura and Chakhirli-Gabala orthogonal faults zone (Fig.2).

Seismo-magnetic effect created by Imishli earthquake has been observed by modern magnetometers installed at seismological stations operating in the Middle Kura depression. The character of the observed seismo-magnetic effect shows that the compressive action is the leading process in the earthquake source and as a result, there has been a reverse deformation and the tension gradient of the geodynamic field has been reduced to positive, but not negative. However, there is an increase of 15-20nT in the seismo-magnetic effect of the magnetometer operating in the Lankaran station 7-8 days before the Imishli earthquake. Analogical situation has been recorded at the Sheki magnetometric variation station. It is also observed that the effect is formed by an increase of 15-20 nT before the earthquake 7-8 days with the same. It is recorded that the seismomagnetic effects were observed with decreases earthquake time and after earthquake at both

stations. Also a detectable seismo-magnetic effect is considered as a key factor in the defining criteria of dependence of the parameters and mechanism of the earthquake sources (Fig. 3) [3].

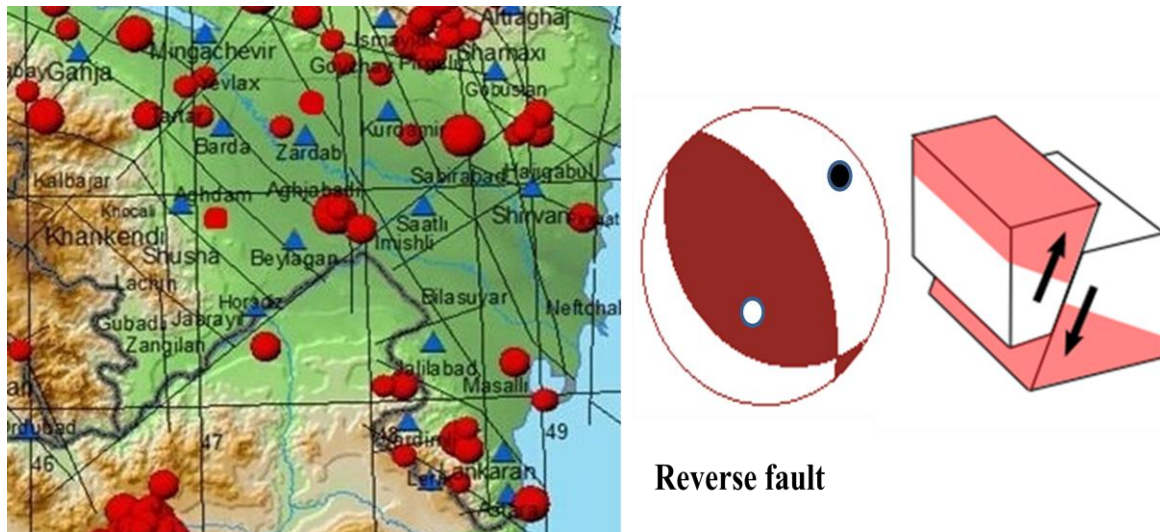


Figure 2. Block-scheme of the displacement and source mechanism of earthquakes occurred in Imishli on 01.08.2016. (compiled by S.E. Kazimova)

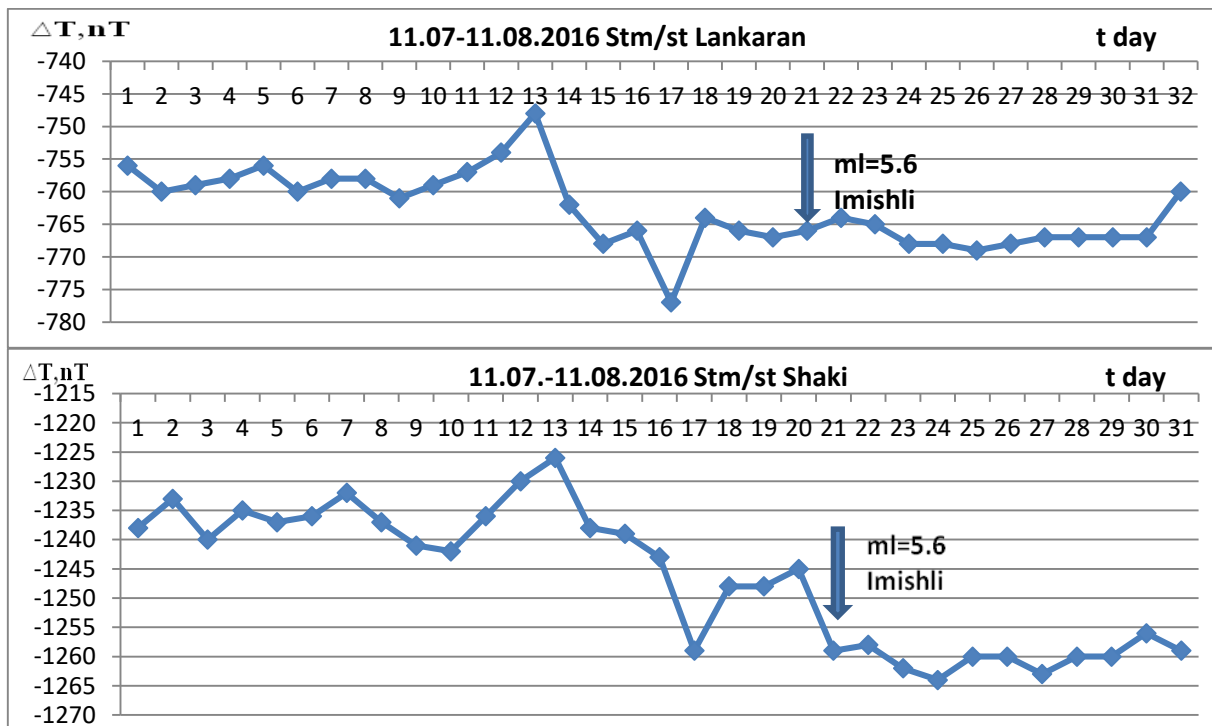


Figure 3. The observed seismomagnetic effect during the Imishli earthquake (ml=5.6, 01.08.2016)

As can be seen from the comparative analysis of the earthquake mechanism and parameters with the curves for the change of seismomagnetic effect, the regularity formed by increases of seismic effect did not justify itself in this episode if the energy of stress-strain in the earthquake source obtained by statistical data for many years is compressive. A similar situation has been reflected during the comparative analysis of the earthquake mechanism and parameters ($H=48$ km, $m_l=5.3$) occurred in Saatly on 11.05.2017 with the variation for the change of seismomagnetic effect. Even though the stress-strain condition is compressive here too, it is noted that the seismomagnetic effect is observed by the decreased during earthquake.

An analysis of the variations of geomagnetic site tension and gradient increases has been allowed us to detect the stress-strain zones in the Middle-Kura depression and adjacent areas. These

are Saatly, Barda, Aghdam, Ujar and Zardab long-term stress-strain zones. In these areas, strong earthquakes are not always present, but are considered as seismic hazard zones and the seismomagnetic effect is observed by anomalous changes [4].

If you look at the map in 2D and 3D format which reflects the stress-strain condition of the geological environment based on magnetic data at the NearKura-Talish geodynamic polygon in 2016 year, the magnetic maximums are recorded in the regional plan (Fig.4).

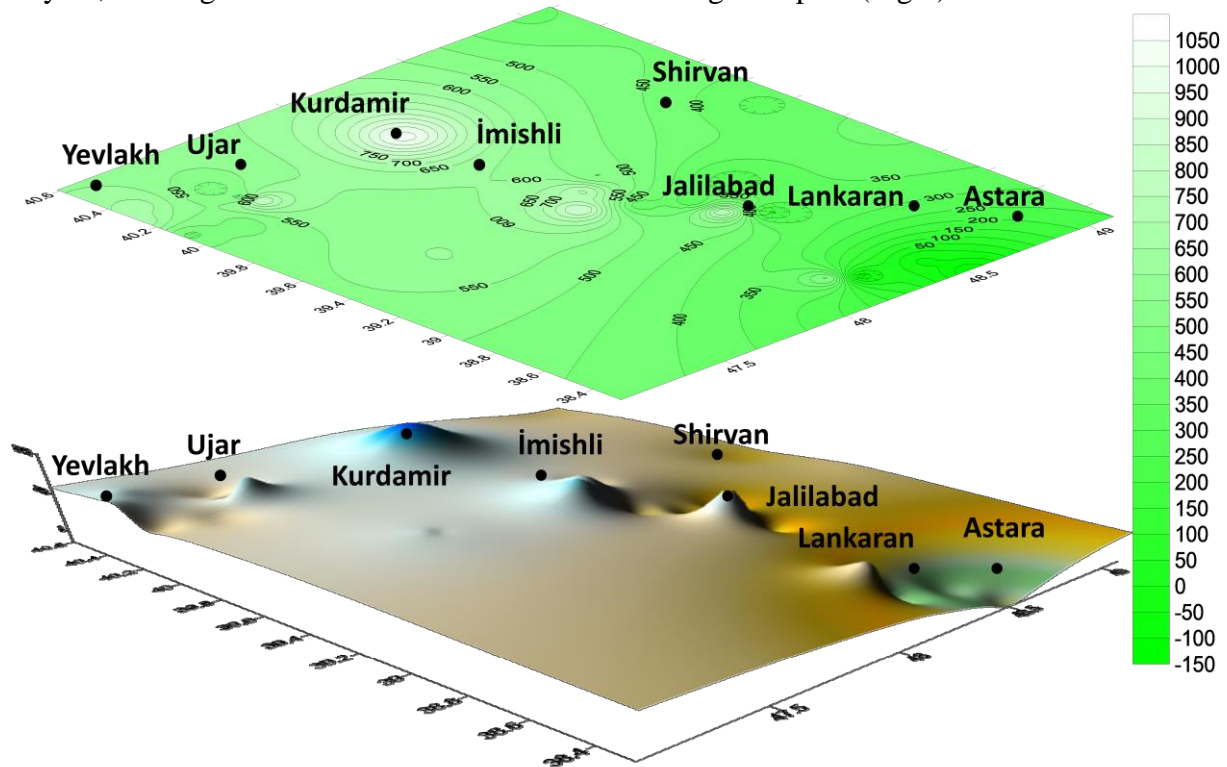


Figure 4. The stress-strain condition of the geological environment on the basis of magnetic data at the Near Kura-Talish polygon (2D, 3D format)

However, in the local area Jalilabad-Imishli and Imishli-Kurdamir maximums are being to the south-east and north-west directions, intensity is 800 in the isolines reflecting the geomagnetic field in the center of the first maximum but to the edges it is 650nT and in the second maximum, these numerals are recorded in the closed form with the intensity 950-650 nT. This situation is reflected in the more complete map in 3D format [5].

The seismoanomal effect in the magnetic field of the Imishli earthquake source zone is determined by the geodynamic regime of the area. It is noted that, geodynamic regime of the Middle Kura depression is related mainly to passed to the bottom of the main blocks of Kura depression to Great Caucasus structure, which is observed by the movement with the south direction of the Great Caucasus structures mentioned in the upper part of the Earth's crust. For this reason, compression deformation occurs in the environment and the seismicity of the area is clarified. [3] The formation of a positive seismomagnetic effect in the Imishli earthquake source zone confirms once again the above mentioned facts. 1

REFERENCES

1. Yetirmişli Q.C. Aşağı Kür çökəkliyinin seysmotektonik şəraiti və onun neftlilik-qazlılıqla əlaqələri. Azərbaycanca Geofizika Yenilikləri Jurnalı. 2000. Bakı.3-4. Səh. 45-49.
2. Велиев Г.О. 1989. Вариации геофизических и геохимических полей в Шемаха-Исмаиллинской сейсмоактивной зоне. Газо-геохимические методы поисков полезных

ископаемых в Южно-Каспийской впадине и обрамляющих горных системах /ГГМ-III/ 15-17 ноября. 1989 г., Баку, с. 143-144.

3. Рзаев А.Г., Етирмишли Г.Д., Казымова С.Э. 2013. Вакı. Отражение геодинамического режима в вариациях напряженности геомагнитного поля. Хəбərləg. Yەر Elmləri, N4, page 3-15.

4. Рзаев А.Г. Связь аномальных изменений в напряженности геомагнитного поля с сейсмотектоническими процессами в литосфере Земли. АМЕА хəбərləg Yەر Elmləri, №32006с, 58-63(рус).

5. Дадашев Ф.Г., Метакса Х.П., Велиев Г.О. 1985. Изучение связи пространственно-временных вариаций геомагнитного поля с сейсмичностью в Исмаиллинской очаговой зоне. Изв. АН Азерб. СССЗ, Наук о Земле, №4, с. 107-112.

6. АМЕА-nın nəzdində RSXM-nin Seysmoloji bölməsinin 2016-cı il hesabatı. АМЕА-nın nəzdində RSXM-nin fond materialları, Bakı 2016.

GEODYNAMIC SITUATION IN AZERBAIJAN ACCORDING TO GPS STATIONS IN 2019

I.E. Kazimov¹

INTRODUCTION

The Global Positioning System (GPS) has provided a new opportunity for direct observation of modern movements and deformations of the Earth's crust, as well as seismic-ionospheric disturbances. GPS studies helped quantify regional deformation in the plate interaction zone [12, 13, 15, 16, 18, 20, 21 and 24]. Regional studies of plate movement use fault orientation, local observations, and restrictions on the relative movement of plates.

The Eastern Mediterranean and the Caucasus are located among Eurasian, African and Arabian plates with complex tectonic activity, for example, volcanic eruptions, mountain building and a significant part of all earthquakes (Fig.1) [17].

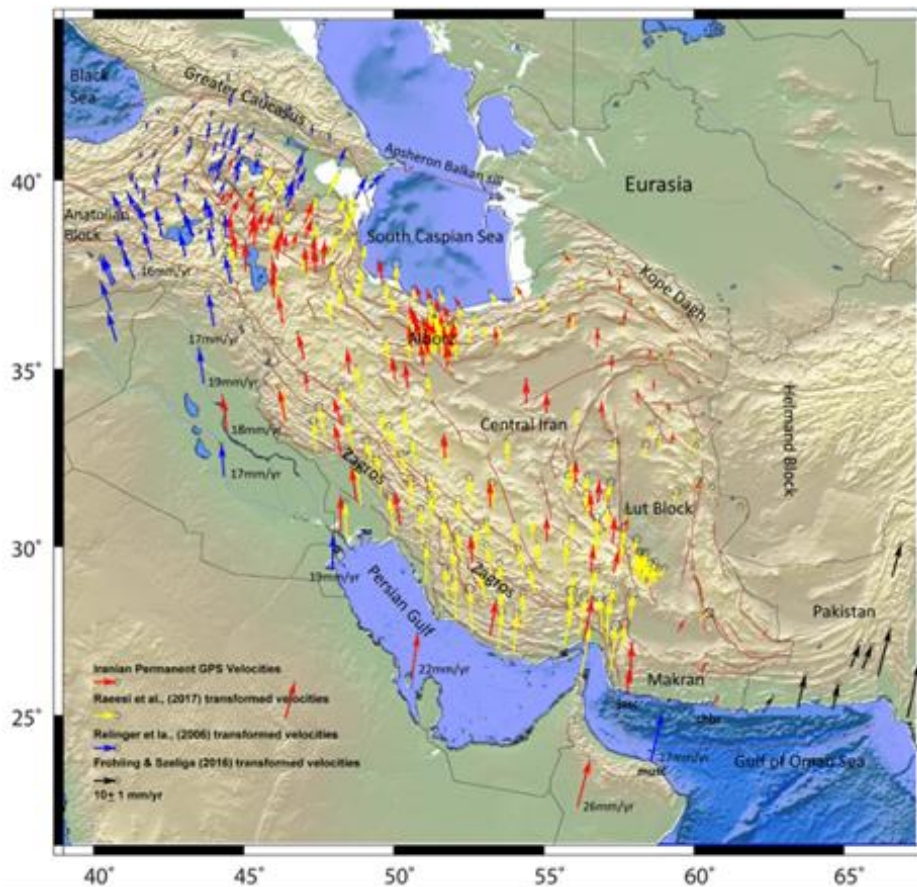


Figure 1. Map of the distribution of vectors of horizontal movements of the Mediterranean and the Caucasus [12] (Unified GPS velocity field relative to the Eurasia fixed frame. Reilinger et al. (2006; blue arrows), Frohling&Szeliga (2016; black arrows) and Raeesi et al. (2017; yellow arrows) velocity fields were transformed into the reference frame of IPGN (red arrows). Major faults of Iran, East Turkey and Caucasus are adapted from Hessami et al. (2003), Ghods et al. (2015) and Talebian et al. (2013)).

The East Anatolian Fault, the Caucasus, and the Zagros Mountains are active continental collision zones due to modern tectonic conditions and structures. The Eastern Mediterranean is one of the important regions for understanding fundamental tectonic processes, such as continental rift genesis, passive margin, subduction and accretion, collision and post collision [11]. These general processes are, in principle, investigated for large areas of the continental lithosphere in order to predict whether the region is seismic and not deformed at present. The tectonic perception of plates

¹ Republican Seismic Survey Center of Azerbaijan National Academy of Sciences

gives a description of continental deformation. The eastern Mediterranean focuses on connecting the Arabian, Eurasian, and Anatolian plates west of the convergence zone. The collision of Saudi Arabia with Eurasia is reduced in the zone of the lithosphere within the deforming region [2, 8].

According to these reconstructions, the Arabian plate advanced 200-600 km from its original place to the place where the continental Eurasian lithosphere was previously located.

As you know, Azerbaijan is part of the Alpine-Himalayan mountain belt formed in the Cenozoic on the southern edge of the East European platform as a result of a collision between the Eurasian and Arabian plates and survived a rapid rise over the past five million years. This work is devoted to the study of the strain rate of the Earth's crust in the territory of Azerbaijan according to GPS observations and its relationship with seismicity. [12, 13]

Tectonics of the studied region

The ongoing “invasion” of the Arabian Plate into Eurasia leads to a reduction in the lithosphere along the Main Caucasian Thrust (MCT), extending in the direction of SW-NE [2, 7, 17]. These regional tectonic processes, being the cause of the deformation of the Earth's crust, cause earthquakes that are historically recorded throughout the Caucasus.

As mentioned above, the territory of Azerbaijan is located in the zone of active collision of two plates, African and Eurasian. Reconstruction of plate tectonics indicates that the collision of the Arabian plate with the Eurasian plate lasts 10-30 million years, right up to the present stage. The speed of movement of the Arabian Plate to the north relative to Eurasia since the beginning of their collision is more or less constant and equal to approximately 20 mm/year [6, 9, 10, 16, 17].

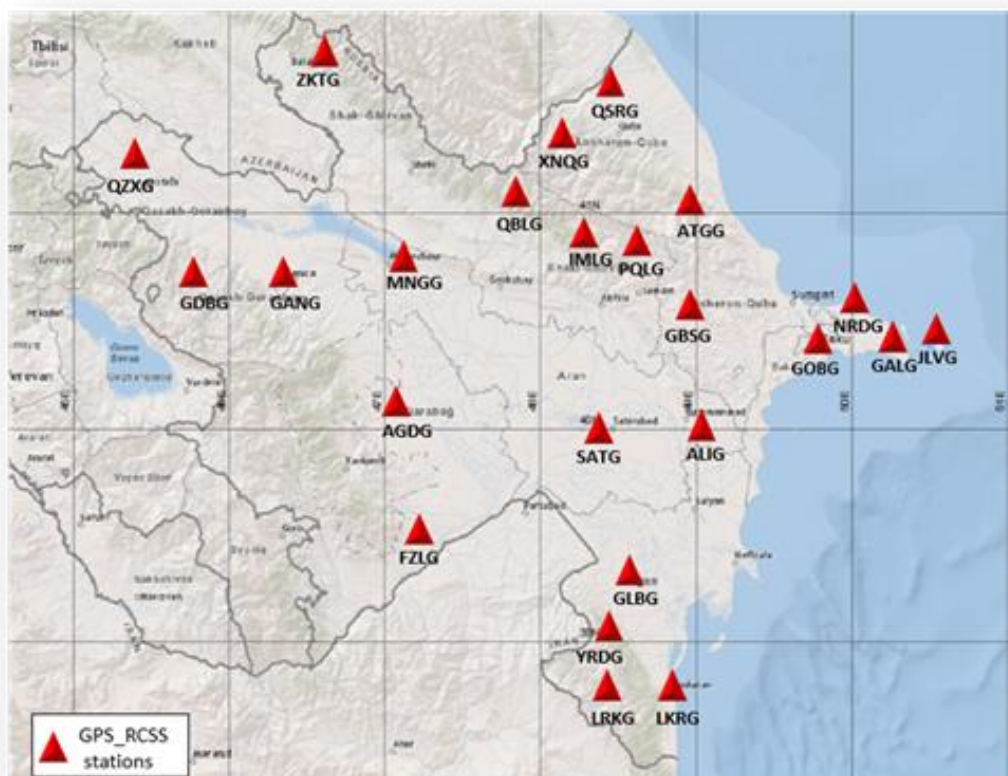


Figure 2. Network of GPS stations in Azerbaijan

Iran's modern tectonics is the result of convergence between north and south among relatively undeformed territories in the southwest (Arabia) and northeast (Eurasia). The NUVEL-1 A global plate motion model predicts a convergence rate of 3–3.5 cm/year. The deformation of Iran includes intracontinental shortening, with the exception of its southeastern margin (Makran), where the oceanic lithosphere of Oman is subducted northward under southeastern Iran (Fig. 1). Within Iran,

most of the deformation probably occurs in the main zones (Zagros, Alborz, Kopetdag) and along large faults that surround the blocks (Central Iranian desert, Loot block and the southern Caspian Sea) with moderate relief and seismicity [17]. The exact distribution of deformation between these tectonic structures is unclear.

Central Iran, Zagros and Makran - this segment of the Alpine-Himalayan belt, lying to the east of the northern ledge of the Arabian Plate.

The Zagros zone, which corresponds to a ridge with a length of up to 1300, a width of 250 and a height of 4.5 km, is formed by a powerful, up to 8-10 km, complex of Paleozoic, Mesozoic and Cenozoic sediments of the passive margin of the Arabian Plate, crushed into large and very long (up to 350 km) folds that gradually change the strike from northwest to east northeast [12].

GPS stations data analysis

At present, 24 GPS stations function in Azerbaijan. The network was created in 2012 (Fig. 2). The network geometry and the location of the measurement points were determined based on the neotectonic structure of the region to characterize as much as possible the relative displacements of the individual elements of this structure and the general deformation of the Earth's crust [3, 4].

GPS data analysis was performed using the GAMIT (version 10.05; Kingand Bock 2001) and GLOBK (version 10.0; Herring 2001) software in the three-step approach described by Feigletal. (1993) [20, 21]. The basis for the velocity estimation is an analysis of the time series of GPS station coordinates calculated from the primary data, which are sets of phase and code measurements at two frequencies lasting 24 hours with a recording interval of 15 s. To assess the speeds of the stations being determined, it is necessary that the network has at least one reference point, and preferably several. We included in this analysis 11 nearby IGS network reference stations: ARTU (Artie, Russia), CRAQ (Simeiz, Ukraine), TEHN (Tehran, Iran) POLV (Poltava, Ukraine), MDVJ (Mendeleyevo, Russia) ANKR (Ankara, Turkey) NICO (Nicosia, Cyprus) DRAG) POL2 (Bishkek, Kyrgyzstan) YIBL (Yibal, Oman) BZGN (Bazergan, Iran) [5] with positions and speeds in ITRF2000 as connecting links with the global reference system (Table 1).

We used the Earth rotation parameters IERS (International Earth Rotation Service) and applied the antenna phase center models depending on azimuth and elevation, following the tables recommended by IGS. Figure 3 shows a map of the distribution of vectors of horizontal movements for 2019. The arrows in the Figure show the direction of the velocity vectors, and the values of the velocities are characterized by the length of the arrows according to the scale shown in the lower right corner of the map. In addition, in Fig.4 shows the temporal variations in the amplitude fluctuations of GPS stations for 2019.

In addition, a speed map of horizontal movements of the geodetic network of GPS stations of Azerbaijan for 2019 was built (Fig. 5). As an analysis of the distribution of speeds shows, the average values of the speeds of horizontal displacements of points to the north and east are not constant, and the processes of shortening the surface of the Earth's crust are also not constant in the study region.

The error in determining the speed varies mainly in the limit of less than 0.6 mm/year, which allows a fairly accurate estimate of the convergence of plates across the Caucasus mountain system (i.e., the error is 5% of the total convergence rate). As one of the main sources of GPS positioning errors, ionospheric delays play a very important role in data processing. Since it is difficult to accurately model the attenuation of the ionosphere, to prevent the effects of ionospheric delays, almost all GPS data processing programs always use a linear combination without ionosphere (LC), including GAMIT, Bernese, GIPSY and PANDA.

The high-speed field of GPS observations quite clearly reflects the movement of the north-north-east (NNE) direction in Azerbaijan and in the adjacent regions of the Lesser Caucasus relative to Eurasia.

Table 1. Parameters of the world reference stations of the IGS network: (ARTU, CRAQ, TEHN, POLV, MDVJ, ANKR, NICO, DRAG, POL2, YIBL, BZGN).

IGS_GPS	region	country	Long,°	Lat,°	reciver	antenna	satellite
ANKR	Ankara	Turkey	39,88	32,75	LEICAGR 30	LEIAR10 NONE	GPS GLONASS Galileo BeiDou SBAS
ARTU	Artie	Russia	56,43	58,56	ASHTECH Z-XII3	ASH700936D_ M + DOME	GPS
CRAO	Simeiz	Ukraine	44,41	33,99	ASHTECH UZ-12	ASH701945C_ M + SCIS	GPS
DRAG	Mezoke	Israel	31,59	35,39	JAVAD TRE_3 DELTA	ASH700936D_ M + SNOW	GPS GLONASS
MDVJ	Mendele yevo	Russia	56.02	37.21	TPS NETG3	JPSREGANT_D D_E1 + NONE	GPS GLONASS
NICO	Nicosia	Cyprus	35,14	33,4	LEICA GR25	LEIAR25.R4 + LEIT	GPS GLONASS Galileo BeiDou SBAS
POL2	Bishkek	Kyrgyzstan	42,68	74,69	ASHTECH UZ-12	TPSCR.G3 NONE	GPS
POLV	Poltava	Ukraine	49,6	34,54	LEICA GR10	LEIAR10 NONE	GPS GLONASS Galileo
TEHN	Tehran	Iran	35,7	51,33	TRIMBLE NETR9	TRM57971.00 + NONE	GPS GLONASS
YIBL	Yibal	Oman	22,18	56,11	TRIMBLE NETR9	ASH701945C_ M + NONE	GPS

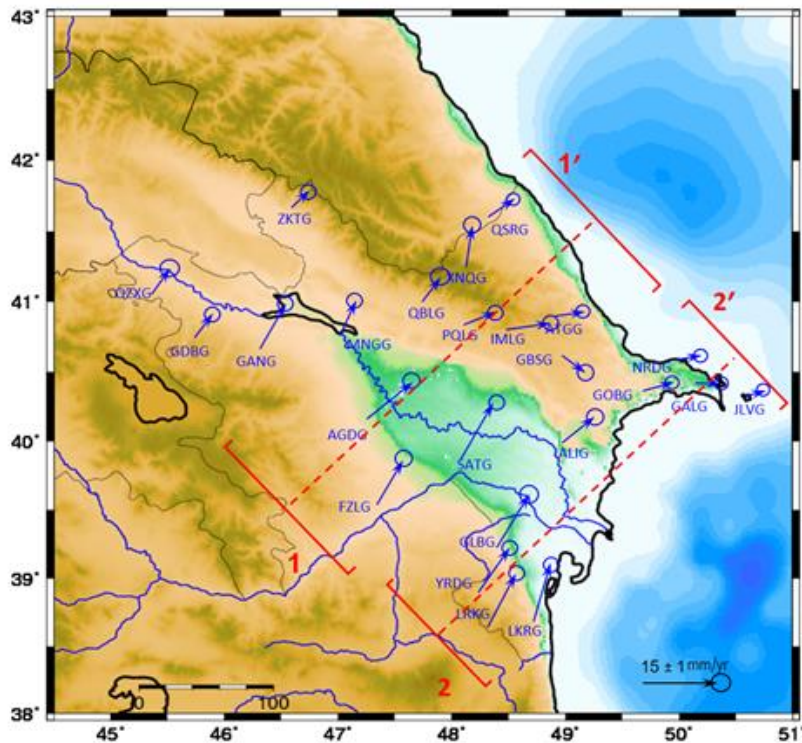


Figure 3. Map of the distribution of vectors of horizontal movements for 2019

The arrows in the Figure show the direction of the velocity vectors, and the velocity values are characterized by the length of the arrows according to the scale shown in the lower right corner of the map. Arrows represent the horizontal station velocities in mm/year referred to the ITRF2008 reference frame. Error ellipses were calculated to the 95% confidence interval.

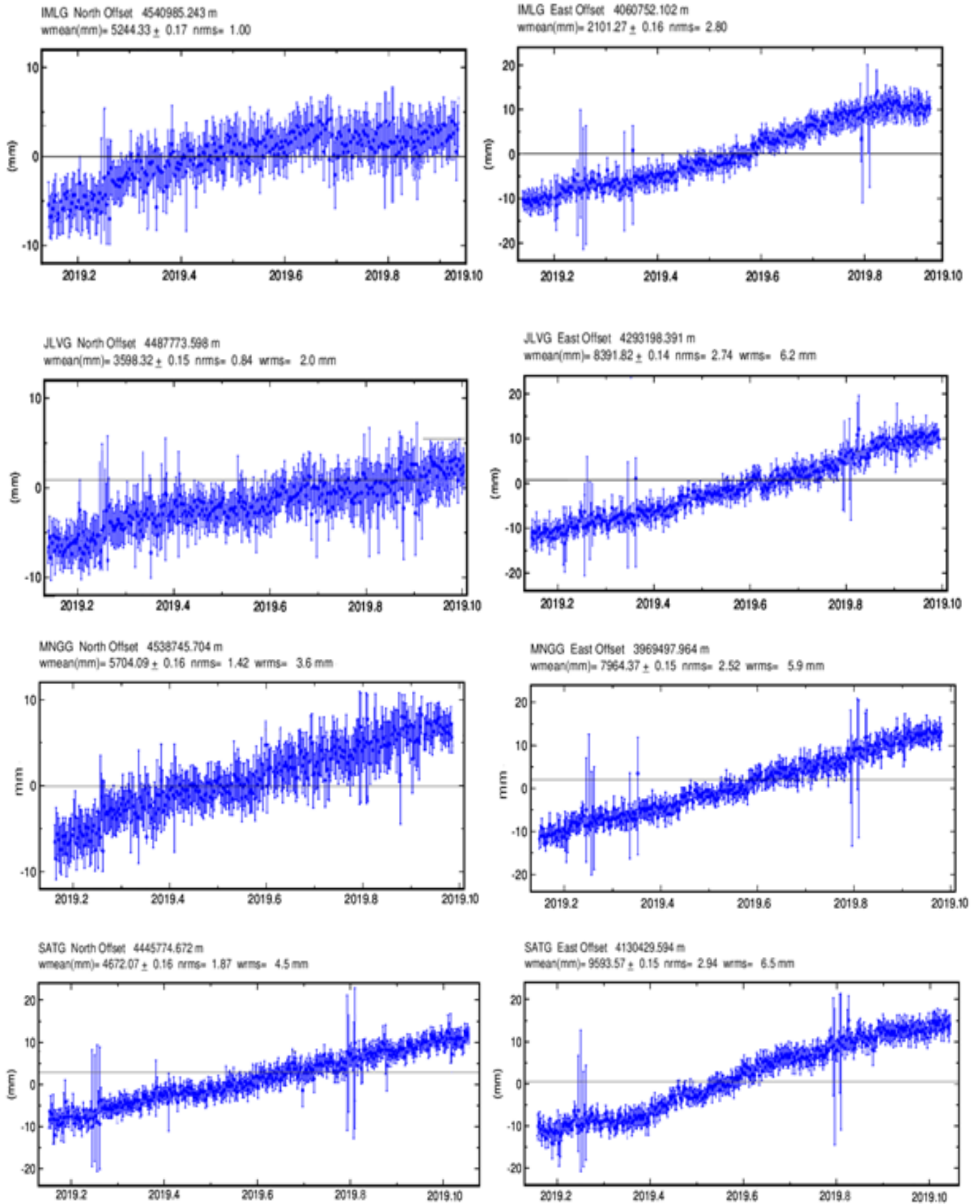


Figure 4. Temporal variations in the amplitude fluctuations of GPS RSSC (IML, JLV, SAT, MNG) stations for 2019.

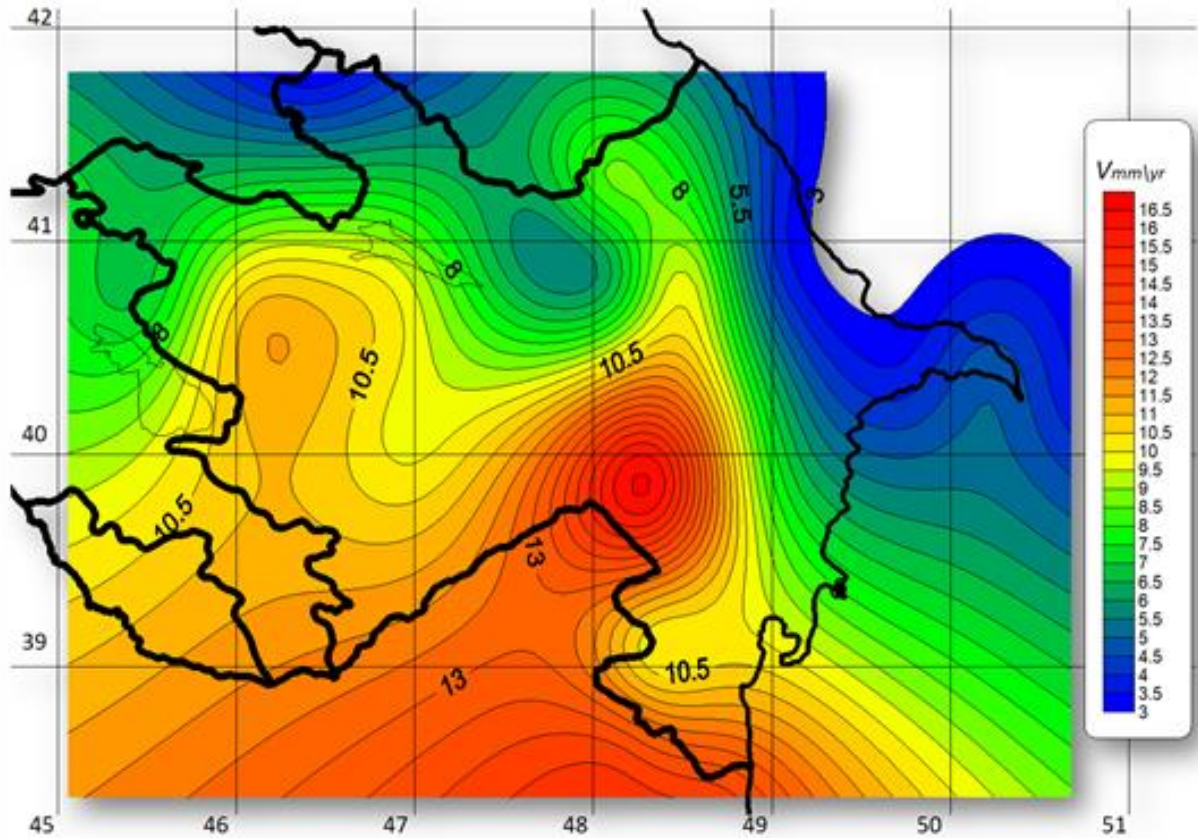


Figure 5. Speed of horizontal movements according to the network of GPS stations of Azerbaijan for 2019.

Table. 2. Coordinates and speeds of horizontal displacements of GPS stations of the territories of Azerbaijan according to profile 1-1

N	coordinates		VEvel(mm/yr)	VNvel.(mm/yr)	AZM , °	V vel(mm/yr)	GPS RSSC stations
	Long,°	Lat,°					
1	48.94	40.54	5.24	-3.88	127	6.5	GBSG
2	48.94	40.86	5.02	0.63	83	5.1	ATGG
3	48.59	40.79	9.26	2.34	76	9.6	PQLG
4	48.39	39.94	7.91	14.52	29	16.5	SATG
5	48.26	41.52	5.32	4.63	49	7.1	QSRG
6	48.18	40.79	5.85	2.62	66	6.4	IMLG
7	48.14	41.17	0.42	8.36	10	8.4	XNQG
8	47.84	40.95	2.96	4.81	32	5.6	QBLG
9	47.32	39.46	5.92	10.5	29	12.1	FZLG
10	47.11	40.11	6.13	7.69	47	9.8	AGDG

The discussion of the results

The GPS observation speed field clearly illustrates the movement of the Earth's crust in the north-west direction in Azerbaijan and related regions of the Lesser Caucasus relative to Eurasia. The most explicit feature of the velocity field is the decrease in speed at the observation points located perpendicular to the Main Caucasian Thrust (MCT) (i.e., at the stations PQLG, XNGG, ZKTG, ATGG, IMLG and GBLG). GPS observation points located along the MCT show a decrease in speed in a westerly direction. N-NE motion of the Earth's surface is interpreted as one of the reasons for the accumulation of stresses on this thrust. In addition, there is a tendency of

horizontal movement within the Kura Depression and the Lesser Caucasus, where the speed increases from west to east along the strike of the mountain range.

In order to clarify the nature of GPS velocities in the seismic zones of the Kura Depression, profiles 1-1' and 2-2 were constructed in the strike cross of the Greater and Lesser Caucasus, as well as in the direction from the Talysh region to the Absheron Peninsula (Fig. 6-7). Table (2-3) presents the coordinates and speeds of the horizontal displacements of GPS stations in Azerbaijan.

Table. 3. Coordinates and speeds of horizontal displacements of GPS stations of the territories of Azerbaijan according to profile 2-2

N	coordinates		VE vel(mm/yr)	VN vel.(mm/yr)	AZM , °	V vel(mm/yr)	GPS stations
	Long,°	Lat,°					
1	50.58	40.31	3.43	1.2	81	3.6	JLVG
2	50.16	40.41	4.8	-0.4	95	4.8	GALG
3	49.99	40.58	3.77	1.13	73	3.9	NRDG
4	49.73	40.40	3.55	0.85	77	3.7	GOBG
5	49.01	39.96	6.09	5.55	48	8.2	ALIG
6	48.78	38.71	4.15	13.23	17	13.9	LKRG
7	48.39	39.24	-1.97	5.01	21	10.2	GLBG
8	48.34	38.64	6.16	13.36	25	14.7	LRKG
9	48.24	38.91	7.18	11.49	32	13.5	YRDG

On the 1-1' profile in the strike cross of the Greater and Lesser Caucasus, there is a noticeable decrease in the speeds of horizontal movements at an epicentral distance of 50 km (Fig. 6), which indicates the approach of the Lesser Caucasus to the Kura Depression at a speed of 12-16 mm/year and a gradual shift of Kura Depression under the Greater Caucasus.

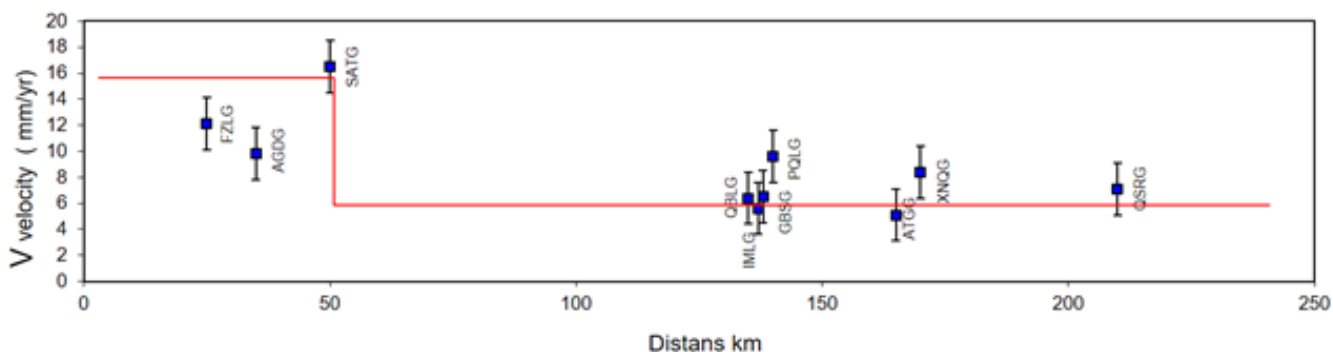


Figure 6. Components of the speeds of horizontal movements of GPS observation points along profile 1-1

In Figure, the profile is shown in the direction from the Talysh region to the Absheron peninsula (SW-NE direction). The speeds of the stations Nardaran, Gobu, Gala and Zhiloy Island, which are included in the Absheron zone, are characterized by almost similar displacement rates (5.3 mm/year, 4.7 mm/year, 4.5 mm/year, and 4.4 mm/year, respectively). The profile shows a noticeable decrease in the northern component of the displacement rates compared to the high values of points located in the southwestern part of the selected profile (LKRG_GPS=13.4 mm/year, GLBG_GPS=13.4 mm/year, YRDG_GPS=12.0 mm/year). In addition, there is a

noticeable increase in the azimuthal angles of the Absheron stations indicating a clockwise movement in the east-south-east direction to 130°.

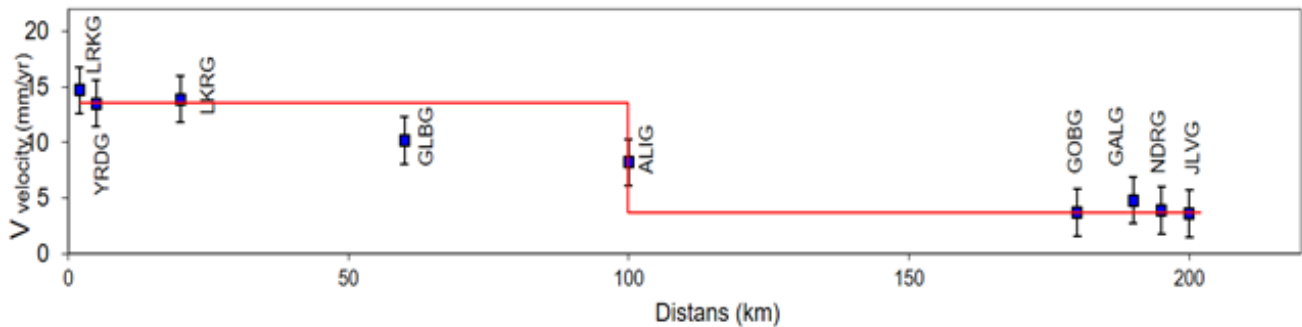


Figure 7. Components of the speeds of horizontal movements of GPS observation points along profile 2-2

At points located in the Lesser Caucasus and the Kura Depression within eastern Azerbaijan, a GPS station located in the coastal zone of the Caspian Sea slightly south of the Absheron Peninsula; there is a sharp decrease in speeds in points and rotation of velocity vectors in the clockwise direction. A sharp decrease in the velocity and rotation of the vectors occurs east of the longitude 40°E along the West Caspian Fault and on the West Caspian Fault a right-side shear movement occurs at a speed of 14 ± 1 mm/year. The existing distribution of velocities and their gradients causes various values of stress accumulation along the MCT, which may affect the seismic mode of the study area.

Conclusion

Detected increase in speed in 2019 at Lerik, Lankaran, Jalilabad, Agdam and Saatli stations, it is the most significant feature of the velocity field in the region where the crust decreases across the eastern MCT segment (longitude 48°). In western Azerbaijan, a reduction in the size of the Earth's crust in the Greater Caucasus occurs between the MCT and the southern wing of the North Caucasian Thrust (NCT).

It was established that along the Kura Depression in the direction from the Middle Kura Depression to the Lower Kura Depression (i.e., from northwest to southeast), a gradual increase in the speeds of horizontal movements from 7.3 to 15.5 mm/year is observed, which is characterized by the compression condition. Note that over the past year, the zone of the Lower Kura Depression is characterized by the manifestation of high seismic activity, expressed in several earthquakes with magnitudes greater than 5, characterized by a reverse fault type.

In addition, a noticeable decrease in horizontal movement speeds at an epicentral distance of 65 km is observed in the strike cross of the Greater and Lesser Caucasus, which indicates the thrust of the Lesser Caucasus on the Kura Depression with an average speed of 10-12 mm/year and the gradual shift of the Kura Depression beneath the Greater Caucasus. On average, in the territory of the Greater Caucasus, at different stations, it was 3.1–9.6 mm/year, and in the Lesser Caucasus, 7–10.1 mm/year.

At GPS stations Nardaran, Gobu, Gala and Zhiloy Island, which are part of the Absheron zone, almost similar values of horizontal displacement velocities are observed (3.9 mm/year, 3.7 mm/year, 4.8 mm/year, and 3.6 mm/year, respectively). In the direction from the Talysh region to the Absheron peninsula (SW-NE direction), a noticeable decrease in the northern component of the displacement rates is observed compared to the high values of the points located in the southwestern part of the selected profile Lerik, Lankaran, Yardimly (14.7 mm/year, 13.9 mm/year, 13.5 mm/year). In addition, there is a noticeable increase in the azimuthal angles of the Absheron stations, indicating a clockwise movement in the east-south-east direction from 40° to 80° -120°.

Thus, based on the data obtained for 2019, the average strain rate in the north-north-east of Azerbaijan is 8.4 mm per year.

REFERENCES

1. Етирмишли Г.Дж., Рзаев А.Г., Казымов И.Э., Казымова С.Э. Моделирование геодинамической ситуации Куринской впадины на основе новейших сейсмологических, геодезических и магнитометрических данных, Бюллетень Оренбургского научного центра УрЦ РАН, 2018, №2, с. 1-11
2. Кадиров Ф.А., Мамедов С.К., Сафаров Р.Т., Исследование современной геодинамической ситуации и опасности землетрясений деформации земной коры территории Азербайджана по 5-летним GPS-данным, Современные методы обработки и интерпретации сейсмологических данных, Обнинск, 2015 г., с. 156-162
3. Казымов И.Э. Геодинамика Абшеронского полуострова, Современные методы обработки и интерпретации сейсмологических данных, Обнинск, 2015 г., с. 163-166
4. Казымов И.Э., Казымова А.Ф. Современная геодинамика Азербайджана по данным GPS станций за 2017-2018 гг., SEISMOPROGNOSIS OBSERVATIONS IN THE TERRITORY OF AZERBAIJAN, Volume 16, № 1, 2019, с 35-42
5. Казымов И.Э., Рахимли З.С., Юзбашиева С.С. Общие принципы обработки спутниковых измерений сети GPS станций Азербайджана, Геофизический институт Владикавказского научного центра РАН Геология и Геофизика Юга России, №1/2017, Владикавказ 2017, ISSN 2221-3198, с 100-114
6. Robert E. Reilinger, Simon McClusky, Philippe Vernant, Shawn A. et.al. GPS constraints on continental deformation in the Africa-Arabia-Eurasia continental collision zone and implications for the dynamics of plate interactions: EASTERN MEDITERRANEAN ACTIVE TECTONICS, journal of geophysical research vol. 111, 2006, DOI: 10.1029/2005jb004051
7. Yetirmishli G.J., Veliyev H.O., Kazimov I.E., Kazimova S.E. Correlation between GPS observation outcomes and depth structure in studying horizontal movements, Бюллетень Оренбургского научного центра УрЦ РАН, 2018, №4, p. 72-85
8. Aktug B., Meherremov, E., Kurt M., Özdemir S., Esedov N., Lenk O., 2013a. GPS constraints on the deformation of Azerbaijan and surrounding regions. J. Geodyn. 67, 40–45.
9. Aktug B., Nocquet J.M., Cingöz A., Parsons B., Erkan Y., England P., Lenk O., Gürdal M.A., Kilicoglu A., Akdeniz H., Tekgül A., 2009. Deformation of western Turkey from a combination of permanent and campaign GPS data: limits to block-like behavior. J. Geophys. Res. Solid Earth 114, B10404.
10. Aktug B., Parmaksız E., Kurt M., Lenk O., Kılıçoğlu A., Gürdal M.A., Özdemir S., 2013b. Deformation of Central Anatolia: GPS implications. J. Geodyn. 67, 78–96.
11. Robertson A., Mountrakis D., 2006. Tectonic Development of the Eastern Mediterranean Region. Geol. Soci. London Spec. Publ. 260, 1–9. Shen, Z.-K., Jackson, D.D., Ge, B.X., 1996.
12. Mahmoud S., Reilinger R., McClusky S., Vernant P., Tealeb A., 2005. GPS evidence for northward motion of the Sinai Block: implications for E. Mediterranean tectonics. Earth Planet. Sci. Lett. 238, 217–224.
13. Mahmoud Y., Masson F., Meghraoui M., Cakir Z., Alchalbi A., Yavasoglu H., Yonlu O., Daoud M., Ergintav S., Inan S., 2013. Kinematic study at the junction of the East Anatolian fault and the Dead Sea fault from GPS measurements. J. Geodyn. 67, 30–39.
14. Masson F., Anvari M., Djamour Y., Walpersdorf A., Tavakoli F., Daignières M., Nankali, H., Van Gorp, S., 2007. Large-scale velocity field and strain tensor in Iran inferred from GPS

- measurements: new insight for the present-day deformation pattern within NE Iran. *Geophys. J. Int.* 170, 436–440.
15. McClusky S., Balassanian S., Barka A., et al., 2000. Global Positioning System constraints on plate kinematics and dynamics in the eastern Mediterranean and Caucasus. *J. Geophys. Res. Solid Earth* 105, 5695–5719.
 16. McClusky S., Reilinger R., Mahmoud S., Ben Sari D., Tealeb A., 2003. GPS constraints on Africa (Nubia) and Arabia plate motions. *Geophys. J. Int.* 155, 126–138. McKenzie D., 1972. Active tectonics of the Mediterranean region. *Geophys. J. Int.* 30, 109–185.
 17. McKenzie D., 1978. Active tectonics of the Alpine—Himalayan belt: the Aegean Sea and surrounding regions. *Geophys. J. Int.* 55, 217–254. McKenzie, D.P., 1970. Plate tectonics of the Mediterranean region. *Nature* 226, 239–243.
 18. Nyst M., Thatcher, W., 2004. New constraints on the active tectonic deformation of the Aegean. *J. Geophys. Res. Solid Earth* 109, B11406. <http://dx.doi.org/10.1029/2003JB002830>.
 19. Regard V., Bellier O., Thomas J.C., Abbassi M.R., Mercier J., Shabanian E., Feghhi K., Soleymani S., 2004. Accommodation of Arabia-Eurasia convergence in the Zagros-Makran transfer zone, SE Iran: a transition between collision and subduction through a young deforming system. *Tectonics* 23. TC4007.
 20. Reilinger R., McClusky S., Vernant P., et al., 2006. GPS constraints on continental deformation in the Africa-Arabia-Eurasia continental collision zone and implications for the dynamics of plate interactions. *J. Geophys. Res. Solid Earth* 111, B05411
 21. Reilinger, R.E., McClusky, S.C., Oral, M.B., King, R.W., Toksoz, M.N., Barka, A.A., Kinik I., Lenk O., Sanli I., 1997. Global Positioning System measurements of present-day crustal movements in the Arabia-Africa-Eurasia plate collision zone. *J. Geophys. Res. Solid Earth* 102, 9983–9999.
 22. Jackson J., McKenzie D., 1984. Active tectonics of the Alpine—Himalayan Belt between western Turkey and Pakistan. *Geophys. J. Roy. Astron. Soc.* 77, 185–264.
 23. Jackson J., Priestley K., Allen M., Berberian M., 2002. Active tectonics of the South Caspian Basin. *Geophys. J. Int.* 148, 214–245. Jin, S.G., Park, P.-H., 2006. Strain accumulation in South Korea inferred from GPS measurements. *Earth Planets Space* 58, 529–534.
 24. Jin S.G., Park P.-H., Zhu W., 2007b. Micro-plate tectonics and kinematics in Northeast Asia inferred from a dense set of GPS observations. *Earth Planet. Sci. Lett.* 257, 486–496.

RESEARCH STUDIES OF THE STRESS-STRAIN STATE AND OF THE SEISMIC RESISTANCE OF UNDERGROUND STRUCTURES

I.R. Sadıgov¹, T.Kh. Aliyev², N.S. Mastanzade³

Underground devices (metro structures, tunnels, water-sewage pipes, reservoirs, etc.) are the most sophisticated devices in mechanics, because these devices are one-way communication devices. What are one-way communication devices? Because the underground facilities are in (surrounded by) the ground the device is operating under influence when force (whether static force or dynamic or seismic force) pushes these devices towards the ground, and when pushed in the opposite direction, the device does not work, i.e. one-way communication is lost. As a result, the rigidity of the device changes. This, as we know, greatly affects the result of the calculation. This calculation has a great effect on dynamic and seismic calculations. In this article, we wanted to review the dynamic and seismic calculations of underground structures. It should be added that in order to solve such complex problems, along with analytical calculations, it is also advisable to conduct experimental testing. In other words, in addition to analytical calculations, it is necessary to apply the experimental method. We have also taken this path in the article. That is, we calculated the underground facility both analytically and experimentally. Dynamic and seismic calculations are based on finding the parameters of the free oscillation of the device. In our opinion, the parameters of the free oscillation of the device (frequency - ν , circular frequency - ω , attenuation - ξ , period - T , etc.) do not depend on external influences. Therefore, the dynamic or seismic motion of a device, as well as its resonance, depends on the overlap of the circular frequency of free movements with the frequency of the circular oscillation of the forced oscillation.

The issue of reducing the risk of seismic collapse has now become the most pressing problem in the theory of earthquake-resistant buildings and structures. Because the following three areas of earthquake protection in seismically dangerous areas are not able to solve this problem unequivocally: 1) Earthquake prevention [2, 3]. This is a natural phenomenon and cannot be prevented; 2) Providing a short-term forecast of the earthquake. Although the method of predicting earthquakes was given by the Japanese scholar Imamuri at the end of the 19th century, it was not possible to implement it successfully, with some exceptions; 3) Although great research has been conducted in the United States, Japan and other countries in the field of calculation, design and construction of earthquake-resistant buildings and structures, in all cases no way has been found to save buildings and structures from earthquakes. Therefore, the opinion of seismologists and anti-seismologists around the world is that the best way to protect against earthquakes and live in harmony with them is to study the risk of seismic collapse.

Determination of seismic risk of groundwater reservoir installation

The Shollar-Baku water pipeline and reservoir, which were a source of pride for Azerbaijanis, scientifically combined with the hydro-technical facilities of the time, and put into operation 100 years ago, are still at the service of people today. This hydraulic installation is indebted to two great historical identity - the great philanthropist, mecenat Haji Zeynalabdin Taghiyev and the English engineer of hydraulic installation William H.Lindley (Sir William Heerleyn Lindley) (Figure 1a).

During the inspection of the reservoir, it was found that there is a need to restore the materials used underground and strengthen the facility [5, 6, 7]. When calculating underground arched structures, the load of the above-ground soil, the horizontal effect of the soil on the walls and the hydrostatic pressure of the water inside are taken into account.

¹ Azerbaijan Architecture and Construction University, Baku

² Azerbaijan Architecture and Construction University, Azerbaijan National Academy of Sciences Republican Seismic Survey Center

³ Research Institute of Building Materials named after S.A.Dadashev

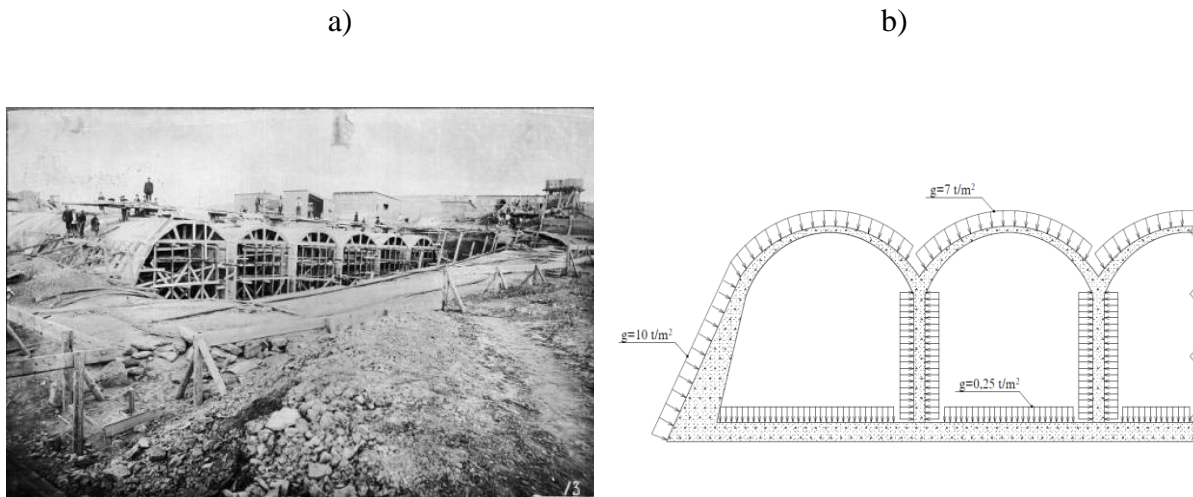


Figure 1. Shollar reservoir during construction (1911) and a fragment of its cross-section with the forces acting on it –b.

Calculation of underground structures by seismic force practically, is a matter of very difficult dynamics. Its exact analytical solution is often not possible. Therefore, numerical methods based on the finite element method are used here. The equilibrium formula of the "ground-device" system for time t can be written as follows:

$$[M]\{U(t)\} + [C]\{\dot{U}(t)\} + [K]\{U(t)\} = \{R(t)\} \quad (1)$$

$\{R(t)\}$ is the vector of external forces; $[M]$ -mass matrix of the system; $U(t)$ -displacement vector; $\dot{U}(t)$ - velocity vector of motion; $\ddot{U}(t)$ - acceleration vector of motion; $[K]$ - stiffness matrix of the system; $[C]$ is the extinction matrix of the system motion. These forms of disintegration lead to changes in the nodes with finite elements and the integration of the dynamic equilibrium state makes it more comfortable. The ground that falls on the arch structure today, newly built reinforced concrete pans and snow load on the arch structure is accepted as $g_1 = 7.0 \text{ tq} / \text{m}^2$. The ground load on the outer walls of the warehouse is $g_2 = 10.0 \text{ tq} / \text{m}^2$. The warehouse floor has a load of $g_3 = 250 \text{ kg} / \text{m}^2$. These are regularly distributed constant loads (Figure 1b). In addition, taking into account the fact that the Baku region is an active earthquake zone, according to the 12-point seismic scale (MSK-64) Here, taking into account the presence of an 8-point zone on a 12-point seismic scale (CEC-64) and the complex engineering and geological conditions and the presence of groundwater, a 9-point seismic zone is adopted, increasing by 1 point according to normative documents [8]. After visual inspection, research was carried out inside the warehouse by non-destructive methods and cern sampling. Considering the aggressive environment inside the reservoir during designing and at that time, due to the low strength and types of steel fittings, the author decided not to use them at all. Thus, for 100 years, very high quality indicators of concrete have emerged. The strength of concrete can be classified as B30 according to today's standards. The design of the warehouse in the form of a vaultin installation elements did not create tension force in its walls but it caused the compression. This caused to the design of the edges of the reservoir at a 45-degree angle and the ground pressure to be regulated by hydrostatic pressure inside the reservoir. From the outside, the outer walls of the warehouse are covered with clay for waterproofing with an average thickness of 1.5 m. Schmidt sclerometer, ferrosan device, georadar instrument, concrete core extraction machine were used during the non-destructive inspection. In addition, engineering and geological surveys were conducted around the warehouse. Geological rocks were drilled at a depth of 10 m, a layer of wastewater was discovered at a depth of 3-7 m. This is confirmed by georadar figures. Later, geo and hydrology condition showed that there are difficult situation in four other reservoirs built in this area in 1930-50 years. Studies in and around these warehouses also confirmed this [5]. Due to the fact that the middle walls of the device are built with low durability

and without reinforcement, they cannot withstand the force of gravity. Therefore, the middle walls of the device are more likely to collapse first. There are 13 such walls in a row. Carbolic band-shaped reinforcement has been proposed to reinforce these walls and the walls of the entire underground reservoir facility in general and extensive experiments have been conducted on such reinforced device fragments [5, 6, 7]. This method of reinforcement has recently become widespread in concrete structures with little or no reinforcement.

Underground iron concrete water-sewage pipes

Underground water-sewage pipes are made of iron-concrete, length is 1-2.5m, with a diameter ranging between Ø600-3000mm, connected to each other in the ground at a depth of 4-6 m. Among the problems in the production of reinforced concrete pipes - achieving the required size of the protective layer of the reinforcement frame in the pipe, the presence of cracks on the pipe and its inner surface, breakage, etc. reduce the time of pipe production. Analyzing the large number of underground pipelines damaged during the earthquake, it can be seen that the main reason is the generation of traction. Iron-concrete pipes are installed only by the method of passing each other and because the distance between the pipes does not exceed 10 cm, there is a danger of the pipes separating from each other due to the transverse force created during landslides and earthquakes. We can give many examples of this (Figure 2). Today, underground iron-concrete water-sewage pipes are produced in iron-concrete plants in special devices by dry vibropressing.



Figure 2. Appearance of pipes damaged during exploitation

The inner and outer surfaces of the pipes coming out of the device are plastered by masters. Groundwater-sewage iron-concrete pipes are strictly accepted in engineering calculations and are calculated according to the scheme without deformation. That is, the reaction of the side ground is not taken into account [10]. It is important to include in the calculation the weight of the pipe and the weight of the water inside, the size of the pipe, the specific gravity of the reinforced concrete and the water. Ground pressure in the vertical direction is assumed to be a uniformly distributed force, and the soil load between the pipe and the ground is assumed to be a variable spreading force. The total value of this force can be written as follows:

$$G_g = \gamma_g H D_e k \quad (2)$$

γ_g is the specific gravity of the soil; H - depth to the pipe at ground level; k - pressure coefficient of soil; D_e - the width of the trench where the pipe is located. The diagram of the forces acting on the pipe is shown in Figure 3.

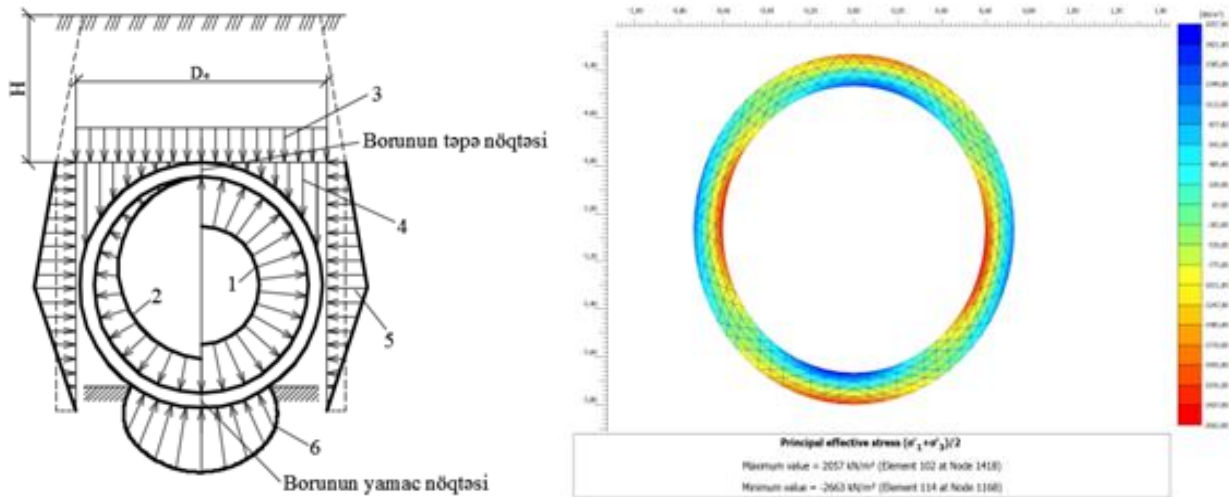


Figure 3. Power scheme affecting the underground pipe (a) and intra-pipe voltage distribution in Plaxis 2D program (b): 1- intra-pipe water pressure; 2 -weight of the pipe; 3-vertival pressure of the upper soil layer; 4-pressure in the upper cavities; 5-edge ground pressure; 6-ground base reaction.

Thus, as soon as four plastic joints are formed in the pipe, the pipe begins to collapse, and it is divided into practically four non-deformable disks. This leads to the propagation of moments along the perimeter of the pipe. PLAXIS 2D computer calculation program was selected for mathematical modeling of the pipe-ground system. This program is used in engineering-geological and design for the analysis of finite element systems. The calculation was carried out under the condition of superficial deformation (Figure 3b) [10]. It should be noted that the tension at the top and slope points of the pipe is mostly on the outer wall of the pipe, but at the middle edge points of the pipe is on the inner wall of the pipe. This indicates that the tension in the compressed areas of the pipe is close to the maximum. The same procedure was calculated on the divisions showing the difference in displacement from the seismic force in the pipes.



Figure 4. Testing of pipes

Pipe tests were carried out on the basis of the Interstate Standard **GOST** 6482-2011 [12]. Therefore, fibrous pipes with a fiber content of 20, 30 and 40 kg/m^3 made by dry vibropressing. In this case, steel reinforcement was completely abandoned in the production of fibroconcrete pipes and reinforcement carcass is replaced by steel and polypropylene fiber. The steel fibers were 6

cm long, 3D-shaped, with 20, 30 and 40 kg of fiber contribution per cubic meter. Polypropylene fibers are added to concrete with a volume of 4 kg/m³. The pipes were stored at the plant until the 28-day concrete strength limit was reached. After collecting the resistance, the pipes were tested in the central laboratory of the plant. The pipe was tested for compressive strength and roof resistance under a hydraulic press (Figure 4) [10].

Each force phase was expected at 2-5 minute intervals, and cracks and deformations in the pipe were observed and recorded. Deformations were recorded by electronic deformation sensors and transmitted to a computer. These sensors were mounted on stationary tripods and recorded the vertical and horizontal deformations of the pipe under the applied force. The tests showed the following results: Maximum force $P_{max} = 123.67\text{kN}$ for 20 kg / m³ fiber contribution, for deformations $\epsilon_y = 15\text{mm}$, $\epsilon_x = 2.5\text{mm}$; for 30 kg / m³ - $P_{max} = 162.50\text{kN}$, $\epsilon_y = 15\text{mm}$, $\epsilon_x = 0.1\text{mm}$; for 40 kg / m³ - $P_{max} = 153.55\text{kN}$, $\epsilon_y = 20\text{mm}$, $\epsilon_x = 4\text{mm}$. The test results are shown in the timetable below. It can be seen that pipes with a fiber content of 30 kg/m³ are the optimal choice. Reduces more fiber addition rates. More fiber addition lowers the indicators.

Table 1

№	The type of pipe being tested, Ø600 mm	Maximum force, kN	Maximum vertical deformation obtained without compression, mm	Enlargement deformation obtained without compression, mm
1	fibroconcrete pipe made of steel fiber with 20 kg/m ³	123,67	15	2,5
2	fibroconcrete pipe made of steel fiber with 30 kg/m ³	162,50	15	0,1
3	fibroconcrete pipe made of steel fiber with 40 kg/m ³	153,55	20	4

a)

b)

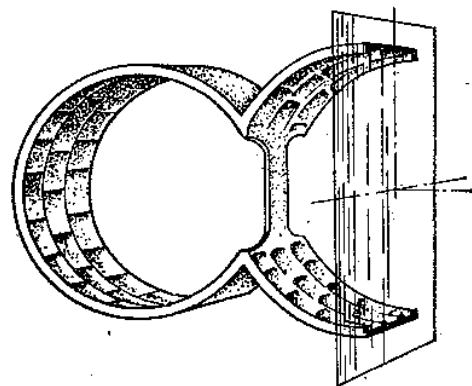
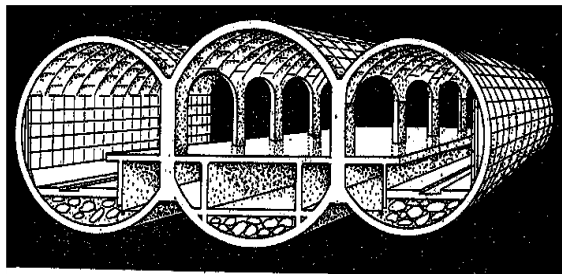


Figure 5. Cross-section of the underground station (a) and typical section for calculation (b) [11]

Calculation, examination and testing of metro facilities

Arch systems have played an important role in the construction of underground facilities. The forces acting on these devices are the weight of the soil on them. These include railway tunnels, underground hydroelectric power stations, metro facilities. A metro station is a complex space device, and a typical section is allocated for its calculation, and it is calculated as a surface system (Figure 5) [10]. In underground installations, the surrounding soil is perceived in the direction of the movement of the installation, and the presence of soil in the opposite direction of the installation should not be taken into account. Thus, the ground is also considered as a one-way communication.

The Winkler model is often adopted as the ground model. The structure that supports the underground structure is called the facing structure. If the ground is unstable, the facing device is built along the entire contour of the device. The facing device is assembled from separate segments. These segments can vary in number from 6 to 9. The segments are made of iron or reinforced concrete. When calculating the subway arch structure, the circular cross section can be shown as a polygon (Figure 6) [11].

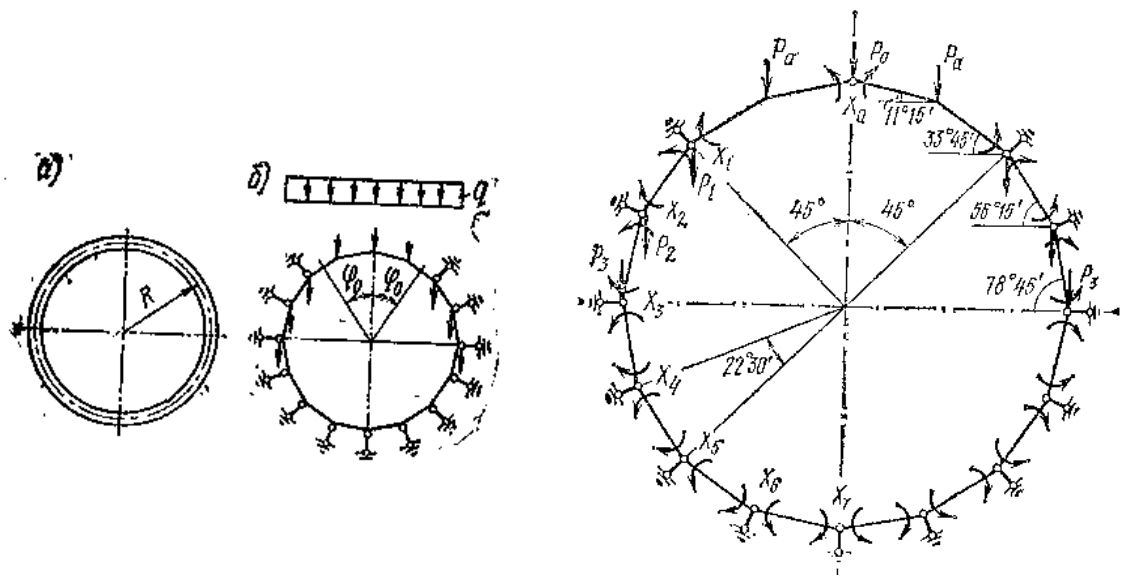


Figure 6. Polygonal scheme of the metro arch installation

The calculation of the facing device can be done more easily in the form of a matrix. Here the force of propagation is replaced by the force at angular points. The surrounding ground is replaced by an unrelated bow system. The stiffness of the bows is calculated as follows:

$$D = kb \frac{s_1 + s_2}{2}, \quad (3)$$

where b is the width of the surface (taken as $b = 1$ in the calculation); s_1 and s_2 are the lengths of the polygon to the right and left of the spring support point; k is the Winkler coefficient of the soil. Today, the biggest problems in the construction of underground subway tunnels are the impact of underground soil on iron concrete elements, moisture in the ground damages the strength of concrete, corrosion of steel reinforcement in segments and eventually loss of element strength. Therefore, as in other facilities, the construction of the subway has already included the construction of fiber-concrete, and its application is on the agenda in many European countries. These studies are based on extensive experimental research and experimental experiments. An example is the application and experimental studies of fibroconcrete segments in Barcelona, Spain (Figure 7) [13].

a)



b)



Figure 7. Iron-concrete segments constructed for a metro installation (a) and its test (b) [13].

In addition, as in any underground facility, different reinforcement methods are used to reinforce other load-bearing elements in metro facilities.

Conclusion and recommendations

1. Knowing the properties of underground structures, it is necessary to know and study the physical and mechanical properties of the soil surrounding the structure - period, extinguishing capacity, density, groundwater level. This issue comes to the fore because "device + enclosed ground" works as a system.

2. Test results of pipes used in underground water supply and sewerage construction have shown a significant advantage of metal and polypropylene fibers in fiber concrete pipes. In particular, modern construction technology, the construction of new metro stations and long-term facilities can have a significant impact on construction that requires compliance with European Standards.

3. Because underground facilities are one-way communication systems, communications are disrupted during an earthquake. This changes the rigidity of the system. Given this situation, it is important to test experimentally to study the true strength and rigidity of the device.

4. Carboniferous tape and laminate surface reinforcement may be offered in case of insufficient or complete reinforcement of steel reinforcement in the reinforced concrete elements of underground facilities.

REFERENCES

1. T.Əliyev. Dinamika (Dinamikanın əsasları və yeraltı qurğuların dinamikası), "Bayatı" sifariş ədəbiyyatı mərkəzi, Bakı, 1994, 214 səhifə.
2. T.X.Əliyev. Seysmik riskin azaldılmasının yeni metodu. Azərbaycan ərazilərində seysmoproqnoz müşahidələrin kataloqu, "Elm" nəşriyyatı, 2011, səh.28-31
3. İ.R.Sadiqov. Materiallar müqaviməti. Dərslik, I hissə, 2010, II hissə, 2013, Bakı, "Təhsil" nəşriyyatı
4. А.П. Синицын Расчет конструкций на основе теории риска. - М.: Стройиздат, 1985.- 304с.,ил.
5. М.Мирзоев, Н.Мастанзаде, Х.Расулов. Вторая молодость Шолларского водопровода. Тандем: Цемент & Строительство. № 2/2013
6. T.Aliyev, N.Mastanzade, M.Mirzoev, Kh.Rasulov, N.Sultanov. Inspection of an Underground Shollar Drinking Water Reservoir and Strengthening of a Design Taking into Account Square

Ecology. *Advances in Ecological and Environmental Research / Science Signpost Publishing.USA. October 25, 2017*

7. T.Əliyev, N.Məstanzadə, N.Sultanov. (2015). Yeraltı Şollar su anbarının karboplastikli armatur liflərlə gücləndirilmiş qurğusunun seysmik riskə düşməsinin üç ölçülü araşdırılması.*Azərbaycanda inşaat və memarlıq. 2(5). 2015*
8. AzDTN 2.3-1. Seysmik rayonlarda tikinti. *Bakı 2010.*
9. СНиП 2.06.08-87. Бетонные и железобетонные гидротехнические сооружения. М.1988
10. Т.Х.Əliyev, N.S.Məstanzadə, Т.М.Рüstəмли. Seysmik təsirdən fibrobeton boruların sonlu elementlər üsulu ilə təhlili. *Azərbaycan Memarlıq və İnşaat Universiteti. Elmi Əsərlər. № 1/2019.*
11. Александров А.В. и др. Строительная механика. Тонкостенные пространственные системы: Учебник для вузов- М. Стройиздат.1983-488 с.ил.
12. ГОСТ 6482-2011. Межгосударственный Стандарт. Трубы железобетонные безнапорные. Технические условия. Москва. Стандартиформ. 2013.
13. A.Fuente, P.Pujadas, A.Blanco, A.Aguado. Experiences in Barselona with the use fibers in segmental linings. *Tunnelling and underground space technology. Ed. C.Rogers and ets. Vol.27, Issue 1, January 2012*

ANNOTATIONS

1. MOHO DEPTH DETERMINATION BY CONVERTED PS-WAVE METHOD FOR THE TERRITORY OF THE GREAT CAUCASUS

S.E. Kazimova

For the first time, based on the analysis of the wave characteristics of distant earthquakes recorded at seismic and telemetric stations of the RSSC, the depths of the Moho border for the territory of the Greater Caucasus were clarified by the method of reflected Ps-waves (Receiver functions). A map of isolines of the depths of the Moho border was constructed and depths were determined for the territory of the Guba-Gusar region 48-50 km, for the Zagatala-Balakan region 46-47 km, for the Shamakhi-Ismayilli region 48-52 km.

Key words: Ps-exchange waves, Receiver function, wave polarization.

2. HYDROGEOLOGICAL CONDITION AND ITS IMPACT ON THE LEVEL OF SEISMIC HAZARD IN NIZAMI DISTRICT, BAKU CITY

Z.S.Aliyeva, L.T.Fettahova, F.Z.Mehdizadeh

It is important to clarify the level of seismic hazard in the construction areas of seismically active areas. One of the major factors that affect the level of seismic hazard is hydrogeological conditions in the construction areas. In order to determine the effect of hydrogeological conditions on the level of seismic hazard, the research works have been carried out in the Nizami district in Baku city. The researches have been carried out mainly based on data materials and well data obtained from the construction fields conducted in the area in 1998-2018.

Key words: hydrogeology, ground, underground water, seismic hazard, point

3. SEISMICITY OF ZAGATALA TERRITORY FOR 2019

S.S. Ismayilova, E.S. Garaveliyev

The seismicity of the Zagatala seismogenic zone has been analyzed on the basis of digital data for 2019. One of the most important events of the year was an earthquake in the Zagatala zone with a magnitude of 4.9.

The Zagatala-Balakan zone is one of the main seismic active zones in Azerbaijan. High seismic activity is observed in the research area in 2019. The article extensively analyzes the history of the area and especially the digital data for 2019. The depth distribution of earthquake epicenters and sources have been studied, the seismic energy allocated by months have been calculated, intensity of the earthquake of magnitude 4.9, that occurred in this area on August 10, 2019, and geometric dimension of the Pleistocene area have been determined on the basis of macroseismic studies.

Key words: seismicity, macroseismic studies, isoseists.

4. FEATURES OF CHANGE OF SEISMOMAGNETIC EFFECTS BEFORE THE STRONG IMISHLI EARTHQUAKE OCCURRED IN THE MIDDLE KURA DEPRESSION IN 2016

N.B. Khanbabayev

Features of seismo-magnetic effect have been studied before tangible Imishli earthquake ($m_l = 5.6$, 01.08.2016). It is noted that the anomalous changes of geomagnetic field stress are preceded by seismic events and reflect the stress-strain condition in the geological environment, as well as the geodynamic process in the source zones.

Key words: ANAS- Azerbaijan National Academy of Sciences, RSSC – Republican Seismic Survey Center, SME- seismo-magnetic effect, nT-nanotesla, mechanism of source.

5. GEODYNAMIC SITUATION IN AZERBAIJAN ACCORDING TO GPS STATIONS IN 2019

Kazimov I.E.

The strain rates of the Earth's crust of the territory of Azerbaijan are considered according to GPS measurements using the GAMIT/GLOBK program for 2019. The axes of compression/contraction of the Earth's crust in the Greater Caucasus region are in the S-NE direction. The maximum values of strain rates (15 mm per year) are observed at stations where there is a sharp change in the directions of the compression axes (SW-NE). Zones with very low strain rates, of 3.6–4.8 mm per year (Absheron Peninsula) were also identified in the deformation field.

Key words: seismicity, GPS, stress state, strain rate, source mechanism.

6. RESEARCH STUDIES OF THE STRESS-STRAIN STATE AND OF THE SEISMIC RESISTANCE OF UNDERGROUND STRUCTURES

I.R.Sadigov, T.Kh.Aliyev, N.S.Mastanzade

The article explores loads on underground structures. The results of experimental tests of the structure to determine the stress-strain state are given on an equal basis with the design methods. In order to increase seismic resistance of structures, versions of carbon fiber reinforcement and structures with steel and polypropylene fiber have been tested as reinforcement.

Key words: stress, strain, fiber concrete, carbon fiber filled.

ANNOTASIYALAR

1. ƏKS OLUNAN PS-DALĞALARIN ÜSULU ƏSASINDA BÖYÜK QAFQAZ ƏRAZİSİNİN MOHO SƏRHƏDİN DƏRİNLİYİN QIYMƏTLƏNDİRİLMƏSİ

S.E. Kazimova

Məqalədə 11 may 2017-ci ildə 07s 24d Saatlı rayonunda və 15 noyabr 2017-ci ildə 23h 48m Ağdam rayonunda baş vermiş güclü 7 bal olan zəlzələlər təhlil olunur. Əsas təkənlərin və onların avterşokların ocaq mexanizmləri qurulub və təhlil olunub. Müəyyən olunub ki, Saatlı zəlzələsi Kür qırılmanın daxilində yerləşir. Ocaqda yerdəyişmənin qiyməti ($DP1=77^\circ$, $DP2=46^\circ$) qırılıb qalxma yerdəyişmə tipli hərəkətlərin üstünlük təşkil etdiyini göstərir. Ağdam zəlzələsi üçün ocaqda yerdəyişmənin qiyməti sol tərəfli yerdəyişmə qırılıb-qalxma tipli hərəkətlər təşkil etdiyini göstərir və Arpa-Samur qırılması ilə uzlaşır.

Zəlzələlərin eninə dalğaların rəqəmsal kanallarının əsasında Furiye spektrləri qurulmuş və bucaq tezliyi f_0 , seysmik momenti M_0 , dairəvi yer dəyişmənin radiusu r_0 , boşalmış gərginlik $\Delta\sigma$, qırılma üzrə yerdəyişmənin qiyməti D və ocağın həcmi V hesablanmışdır.

Açar sözlər: ocağın mexanizmi, qırılıb-qalxma, dairəvi yer dəyişmənin radiusu, qırılma üzrə yerdəyişmənin qiyməti.

2. BAKI ŞƏHƏRİ, NİZAMİ RAYONUNDA HİDROGEOLOJİ ŞƏRAİT VƏ ONUN SEYSMİK TƏHLÜKƏ SƏVİYYƏSİNƏ TƏSİRİ

Z.S. Əliyeva, L.T. Fəttahova, F.Z. Mehdizadə

Seysmik cəhətdən aktiv ərazilərdə tikinti aparılan sahələrdə seysmik təhlükənin səviyyəsinin dəqiqləşdirilməsi mühüm əhəmiyyət kəsb edir. Seysmik təhlükənin səviyyəsinə təsir edən əsas amillərdən biri tikinti sahəsindəki hidrogeoloji şəraitdir. Hidrogeoloji şəraitin seysmik təhlükənin səviyyəsinə təsirini müəyyənləşdirmək məqsədilə Bakı şəhərinin Nizami rayonu ərazisində tədqiqat işləri aparılmışdır. Araşdırmalar əsasən fond materialları və 1998-2018-ci illərdə ərazidə aparılmış tikinti sahələrindən əldə olunmuş quyu məlumatları əsasında aparılmışdır.

Açar sözlər: hidrogeoloji, qrun, yeraltı sular, seysmik təhlükə, bal.

3. 2019-CU İLDƏ ZAQATALA ƏRAZİSİNİN SEYSMİKLİYİ

S.S. İsmaylova, E.S. Qaravəliyev

2019-cu il ərzində Zaqatala seysmogen zonasının rəqəmsal məlumatlar əsasında seysmikliyi analiz olunmuşdur. İl ərzində ən mühüm hadisələrdən biri də Zaqatala zonasında baş vermiş maqnitudası $m=4.9$ olan zəlzələdir.

Zaqatala-Balakən seysmoaktiv zonası Azərbaycanın əsas seysmoaktiv zonalarından biri sayılır. 2019-cu ildə öyrənilən ərazinin seysmik aktivliyinin yüksək olması müşahidə olunur. Məqalədə ərazinin tarixi və əsasən də 2019-cu ildə rəqəmsal məlumatlar geniş təhlil olunmuşdur. Zəlzələ episentrlərinin və ocaqlarının dərinlik üzrə paylanması araşdırılmış, aylar üzrə ayrılan seysmik enerji hesablanmış, 10 avqust 2019-cu il tarixində bu ərazidə baş vermiş maqnitudası $m=4.9$ olan zəlzələnin makroseysmik tədqiqatlar əsasında intensivliyi və pleystoseyst sahəsinin həndəsi ölçüləri müəyyən edilmişdir.

Açar sözlər: Seysmiklik, makroseysmik tədqiqatlar, izoseystlər.

4. ORTA KÜR ÇÖKƏKLİYİNDƏ 2016-CI İLDƏ BAŞ VERMİŞ GÜCLÜ İMİŞLİ ZƏLZƏLƏSİNDƏN ÖNCƏ SEYSMOMAQNİT EFFEKTİN DƏYİŞMƏ XÜSUSİYYƏTLƏRİ

N.B. Xanbabayev

Hiss olunan İmişli zəlzələsindən əvvəl ($m_l=5.6$ 01.08.2016) seysmomaqnit effektin xüsusiyyətləri xarakteri öyrənilmişdir. Qeyd edilir ki, geomaqnit sahə gərginliyinin anomal dəyişmələri seysmik hadisələri qabaqlayır və geoloji mühitdəki gərginlik-deformasiya vəziyyətini, həmçinin ocaq zonalarında gedən geodinamik prosesi əks etdirir.

Açar sözlər: AMEA-Azərbaycan Milli Elmlər Akademiyası, RSXM-Respublika Seysmoloji Xidmət Mərkəzi, SME-seysmomaqnit effekt, nT-nanotesla, ocağın mexanizmi.

5. GPS STANSİYALARININ MƏLUMATLARINA GÖRƏ 2019-CU İLDƏ AZƏRBAYCANDA GEODİNAMİK VƏZİYYƏT

I.E. Kazımov

GPS stansiyaların GAMIT/GLOBK proqramın vasitəsi ilə hesablanan 2019-cu il məlumatları əsasında Azərbaycan ərazisi üçün Yer qabığının deformasiya sürətlərinin təhlil olunur. Böyük Qafqaz ərazisi üçün şimal-şimal-şərq istiqamətli hərəkətlər müşahidə olunur. Ən yüksək sürətlər (15 mm/il) sıxılma oxlarının istiqamətlərində kəskin dəyişiklik (CQ-ŞŞ) olan stansiyalarda müşahidə olunur. Hətəda deformasiya sahədə çox aşağı sürətlə hərəkət edən ərazilər də müəyyən edilib – 3.6-4.8 mm/il (Apseron yarımadası).

Açar sözlər: seysmiklik, GPS stansiyaları, gərginlik vəziyyəti, ocaq mexanizmləri.

6. YERALTI QURĞULARIN GƏRGİN-DEFORMASIYA HALININ ARAŞDIRILMASI VƏ ZƏLZƏLƏYƏ DAVAMLILIĞININ ÖYRƏNİLMƏSİ

İ.R.Sadıqov, T.X.Əliyev, N.S.Məstanzadə

Xülasə: Məqalədə yeraltı qurğularına təsir edən qüvvələr araşdırılmışdır. Hesablama üsulları ilə bərabər eksperimental sınaq yolla qurğuların gərçək gərgin-deformasiya halı tədqiq olunmuşdur. Qurğuların zəlzələyə davamlılıq məqsədi ilə gücləndirilməsində karbolifli səthi armatur, dəmir və polipropilen fibra qatılımı təklifləri yoxlanılmışdır.

Açar sözlər: gərginlik, deformasiya, fibrobeton, karbolifli plastik armatur.

АННОТАЦИИ

1. ОЦЕНКА ГЛУБИНЫ ПОВЕРХНОСТИ МОХО МЕТОДОМ ОБМЕННЫХ PS-ВОЛН ДЛЯ ТЕРРИТОРИИ БОЛЬШОГО КAVKAZA

С.Э. Казымова

В статье анализируются сильные 7-ми бальные землетрясения произошедшие 11 мая 2017 г., в 07h 24m в Саатлинском районе и 15 ноября 2017 г. в 23h 48m в Агдамском районе. Построены и проанализированы решения механизмов очагов основного толчка и наиболее ощутимых афтершоков. Очаговая область Саатлинского землетрясения находится в зоне действия Куринского разлома. Тип движения по обеим крутым плоскостям ($DP1=77^\circ$, $DP2=46^\circ$) – взброс с небольшими элементами сдвига. Эпицентр Агдамского землетрясения приурочен к Арпа-Самурскому разлому и могут быть проинтерпретированы как правосторонняя взбросо-сдвиговая деформация в зоне геодинамического влияния левостороннего Арпа-Самурского разлома. По цифровым сейсмограммам поперечных волн землетрясений были построены амплитудные спектры Фурье, которые дали возможность определения таких динамических параметров, как угловая частота f_0 , сейсмический момент M_0 , радиус круговой дислокации R , сброшенное напряжение D_s , средняя подвижка по разрыву D .

Ключевые слова: механизм очага, взброс, радиус круговой дислокации, средняя подвижка по разрыву.

2. ГИДРОГЕОЛОГИЧЕСКОЕ СОСТОЯНИЕ И ЕГО ВЛИЯНИЕ НА УРОВЕНЬ СЕЙСМИЧЕСКОЙ ОПАСНОСТИ В НИЗАМИНСКОМ РАЙОНЕ, ГОРОДА БАКУ

З.С. Алиева, Л.Т. Фаттахова, Ф.З. Мехтизаде

Одной из важнейших задач в области сейсмостойкого строительства является оценка уровня сейсмической опасности на строительных площадках. При определении условий строительства большое влияние на интенсивность землетрясений оказывают местные инженерно-геологические условия, где особое место занимают гидрогеологические условия. Для оценки влияния гидрогеологических условий на сейсмичность изучаемой территории, в Низаминском районе г.Баку были проведены исследования на основании фондового материала за 20 лет (1998-2018 г.г.) и литературных данных.

Ключевые слова: гидрогеология, грунты, подземные воды, сейсмическая опасность, бал.

3. СЕЙСМИЧНОСТЬ НА ТЕРРИТОРИИ ЗАГАТАЛЫ В 2019 ГОДУ

С.С. Исмайлова, Э.С. Гаравелиев

На основе цифровых данных была проанализирована сейсмичность Загатальской сейсмогенной зоны за 2019 г. Одним из важнейших событий года стало землетрясение произошедшее в Загатальском районе с магнитудой $m_l=4.9$.

Загатала-Балаканская сейсмогенная зона является одной из основных сейсмоактивных зон в Азербайджане. В 2019 году в районе исследований наблюдается высокая сейсмическая активность. В статье анализируется сейсмичность в исторический период и в период использования цифровых данных за 2019 год. Было изучено распределение эпицентров землетрясений как в пространстве так и по глубине, рассчитана сейсмическая энергия по месяцам, интенсивность, а также для сильного землетрясения произошедшего 10 августа 2019 года с магнитудой $m_l=4.9$ были определены геометрические размеры плейстосейстовой области на основе макросейсмических исследований.

Ключевые слова: сейсмичность, макросейсмические исследования, изосейсты.

4. ОСОБЕННОСТИ ИЗМЕНЕНИЯ СЕЙСМОМАГНИТНЫХ ЭФФЕКТОВ ПЕРЕД СИЛЬНЫМ ЗЕМЛЕТРЯСЕНИЕМ В ИМИШЛИ, ПРОИЗОШЕДШИМ В СРЕДНЕ КУРИНСКОЙ ВПАДИНЕ В 2016 ГОДУ

Н.Б. Ханбабаев

Изучен характер проявления сейсмомагнитного эффекта перед ощутимым Имишлинским землетрясением ($m_l=5.6$, 01.08.2016). Аномальные изменения в напряженности геомагнитного поля предвещают сейсмическое событие и отражают напряженно-деформированное состояние геологической среды и геодинамический процесс в области формирования очаговой зоны.

Ключевые слова: НАНА – Национальная академия наук Азербайджана, РЦСС - Республиканский центр сейсмологической службы, сейсмомагнитный эффект, нТл - нано Тесла, механизм очага.

5. ГЕОДИНАМИЧЕСКАЯ ОБСТАНОВКА В АЗЕРБАЙДЖАНЕ ЗА 2019 г. ПО ДАННЫМ GPS СТАНЦИЙ

И.Э. Казымов

Рассматриваются скорости деформаций земной коры территории Азербайджана по данным GPS-измерений на основе программы GAMIT/GLOBK за 2019 год. Оси сжатия/сокращения земной коры в регионе Большого Кавказа имеют Ю-СВ направление. Максимальные значения скоростей деформации (порядка 15мм в год) наблюдаются на станциях, где имеет место резкое изменение направлений осей сжатия (ЮЗ-СВ). В деформационном поле выявлены также зоны с очень низкими скоростями деформации, порядка 3.6-4.8мм в год (Апшеронский п-ов).

Ключевые слова: сейсмичность, GPS, напряженное состояние, скорость деформации, механизм очага.

6. ИССЛЕДОВАНИЕ НАПРЯЖЕННО-ДЕФОРМИРОВАННОГО СОСТОЯНИЯ И ИЗУЧЕНИЕ СЕЙСМОСТОЙКОСТИ ПОДЗЕМНЫХ СООРУЖЕНИЙ

И.Р.Садыгов, Т.Х.Алиев, Н.С.Мастанзаде

В статье исследуются нагрузки, действующие на подземные сооружения. Наравне с расчетными методами приводятся результаты экспериментальных испытаний конструкции по определению напряженно-деформированного состояния. С целью повышения сейсмостойкости сооружений в качестве усиления проверены варианты углепластикового армирования и конструкции с металлической и полипропиленовой фиброй.

Ключевые слова: напряжение, деформация, фибробетон, углепластиковая арматура.

Scope of the Journal

The Journal "Seismoprognosis observations in the territory of Azerbaijan" is specializing on the theoretical and practical aspects of seismology, engineering seismology and earthquake prediction. In the journal are publishing scientific articles on seismology of local and foreign scientists.

The journal is officially registered by the Highest Certifying Commission under the President of Azerbaijan Republic.

The journal publishes scholarly articles on seismology, historical seismicity, seismic source physics, strong-motion studies, seismic hazard or risk, earthquake disaster mitigation and emergency planning, engineering seismology, triggered and induced seismicity, volcano seismology, earthquake prediction, geodynamics, GPS measurements, gravimetric, magnetic and electrometric investigations in seismogenic areas.

Information for Authors

Works will only be considered if not previously published anywhere else and must not be under consideration for publication in any other journal or book. Manuscripts must contain original work and information derived from scientific research projects or technical developments. The ideas expressed by publishing in journal are the sole responsibility of the authors.

Research papers that are selected for in-depth review are evaluated by at least two outside reviewers. Reviewers are contacted before being sent a paper and asked to return comments within 1 to 2 weeks for most papers.

We ask you to send articles for publication in the journal to our e-mail: journal@seismology.az

To submit your manuscript you can use our manuscript submission system also. Please follow the formatting instructions found on this site: <http://seismology.az/journal/pages/rules>

www.seismology.az/journal
25, Nigar Rafibeyli str., AZ1001, Baku, Azerbaijan
Republican Seismic Survey Center
of Azerbaijan National Academy of Sciences
Phone: +994 12 492-34-37;
Fax: +994 12 492-31-65;
E-mail: seys@azeurotel.com;
science@azeurotel.com

CONTENTS

<i>S.E. Kazimova:</i> Moho depth determination by converted PS-wave method for the territory of the Great Caucasus	3
<i>Z.S.Aliyeva, L.T.Fettahova, F.Z.Mehdizadeh:</i> Hydrogeological condition and its impact on the level of seismic hazard in Nizami district, Baku city	10
<i>S.S. Ismayilova, E.S. Garaveliyev:</i> Seismicity of Zagatala territory for 2019	15
<i>N.B. Khanbabayev:</i> Features of change of seismomagnetic effects before the strong Imishli earthquake occurred in the Middle Kura depression in 2016.....	21
<i>I.E.Kazimov:</i> Geodynamic situation in Azerbaijan according to GPS stations in 2019	26
<i>I.R.Sadigov, T.Kh.Aliyev, N.S.Mastanzade:</i> Research studies of the stress-strain state and of the seismic resistance of underground structures	36
Annotations	44

**SEISMOPROGNOSIS OBSERVATIONS
IN THE TERRITORY OF AZERBAIJAN**

Volume 18, № 1, 2020
<http://www.seismology.az/journal>

Director of publishing house: **S.A.Gahramanov**
Editor of publishing house: **Kh.M.Nabiyev**

Format 60x84 ¹/₈
Print 500 copy
Price is under the treaty

Adress: AZ1001, 28 Istiglaliyyat str., Baku